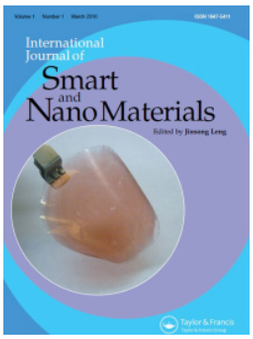

International Journal of Smart and Nano Materials

ISSN: 1947-5411 (Print) 1947-542X (Online) Journal homepage: www.tandfonline.com/journals/tsnm20

Mass transfer strategies for MicroLED chip assembly: pick-and-place techniques and fluidic self-assembly methods

Jinsheng Zhao, Xiangyu Li, Yangmin Li & Lidong Yang

To cite this article: Jinsheng Zhao, Xiangyu Li, Yangmin Li & Lidong Yang (2025) Mass transfer strategies for MicroLED chip assembly: pick-and-place techniques and fluidic self-assembly methods, International Journal of Smart and Nano Materials, 16:2, 359-396, DOI: 10.1080/19475411.2025.2500026

To link to this article: https://doi.org/10.1080/19475411.2025.2500026

Published online: 06 May 2025.

INTERNATIONAL JOURNAL OF SMART AND NANO MATERIALS
2025, VOL. 16, NO. 2, 359–396
https://doi.org/10.1080/19475411.2025.2500026

Taylor & Francis
Taylor & Francis Group

Mass transfer strategies for MicroLED chip assembly: pick-and-place techniques and fluidic self-assembly methods

Jinsheng Zhao[a], Xiangyu Li[b], Yangmin Li[a] and Lidong Yang[a]

[a]Research Institute for Advanced Manufacturing, Department of Industrial and Systems Engineering, The Hong Kong Polytechnic University, Kowloon, Hong Kong; [b]Applied Mechanics and Structure Safety Key Laboratory of Sichuan Province, School of Mechanics and Aerospace Engineering, Southwest Jiaotong University, Chengdu, China

ABSTRACT

Micro light-emitting diode (MicroLED) displays possess exceptional advantages including rapid response speed, autonomous light emission, high contrast, and long service life. The technology is emerging alongside rapid advancements in wearable devices, virtual reality, augmented reality, and TV displays. Due to these strengths, MicroLED displays are widely recognized as the most disruptive and revolutionary next-generation display technology. However, the miniaturized characteristic of MicroLED chips poses significant challenges for efficiently, accurately, and cost-effectively transferring millions of these chips from the donor substrate to the receiver substrate. Over the past two decades, numerous innovative mass transfer strategies have been developed. These strategies aim to overcome the limitations of traditional transfer techniques. Such advancements are driving the commercialization of MicroLED displays. Herein, we review the development of mass transfer strategies for MicroLED chips and classify these strategies into two primary categories: pick-and-place technique and fluidic self-assembly method. The former is further classified based on different adhesion modulation mechanisms, while the latter is classified based on different driving forces. Furthermore, this review provides an in-depth analysis of the working mechanisms, along with a comprehensive evaluation of the advantages and disadvantages associated with specific strategies.

ARTICLE HISTORY
Received 28 February 2025
Accepted 27 April 2025

KEYWORDS
Mass transfer strategy; MicroLED chip; pick-and-place; fluidic self-assembly

CONTACT Lidong Yang lidong.yang@polyu.edu.hk Research Institute for Advanced Manufacturing, Department of Industrial and Systems Engineering, The Hong Kong Polytechnic University, Kowloon 999077, China

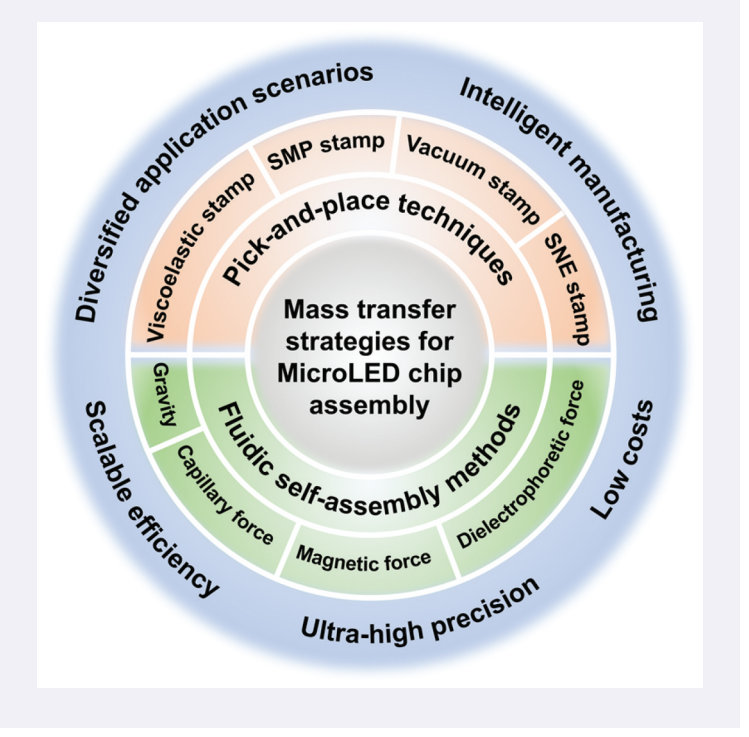

1. Introduction

As a fundamental technology for the development of the modern information society, display technology has experienced rapid advancement [1,2]. From digital watches to virtual reality glasses, and from large-scale video billboards to the micro light-emitting diode (MicroLED) TVs named the Wall [3], the iteration of display technology has significantly transformed social production and modern life [4,5]. The first generation of display technology, the cathode ray tube (CRT) [6], accelerated the emergence and widespread adoption of video displays. However, due to their inability to meet modern requirements for low power consumption and high resolution, CRT displays have gradually been phased out [7]. They have been replaced by liquid crystal displays (LCDs) [8–10] and organic light-emitting diode (OLED) displays [11–14], which have become the two dominant display technologies in contemporary applications [15]. Despite their prevalence, both LCD and OLED technologies exhibit certain limitations [16]. For instance, the slower response time of LCDs results in suboptimal dynamic image performance, while long-term use of OLED displays can lead to screen aging, reduced brightness, and color distortion. In contrast, MicroLED display technology, characterized by its high brightness, self-luminous properties, high resolution, low power consumption, fast response time, and long lifespan, has been hailed as the next-generation mainstream display technology [17].

In the year 2000, Jin et al. pioneered the development of MicroLED chips based on Group III nitrides [18,19], thereby introducing the concept of MicroLED. Over the past two decades, extensive scientific research has significantly propelled the growth of the MicroLED industry [20–31]. A complete manufacturing chain of MicroLED displays

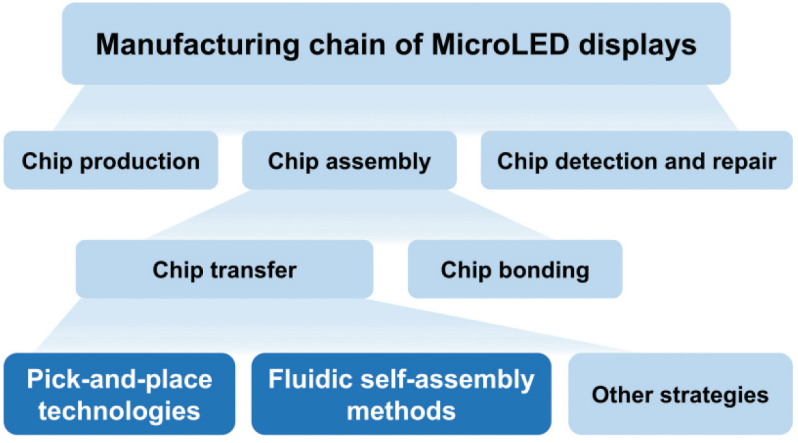

Figure 1. The manufacturing chain of MicroLED displays as well as this paper's focuses on chip transfer technologies, including pick-and-place techniques and fluidic self-assembly methods.

encompasses three critical processes: chip production, chip assembly, and chip detection and repair (Figure 1). However, as commercialization efforts have progressed, numerous technical challenges have become increasingly prominent [32–40]. Among these, the mass transfer technique is currently regarded as the most critical bottleneck [5,41,42].

MicroLED displays utilize multi-colored self-emitting elements, comprising tens of millions of MicroLED chips in red, green, and blue (RGB) colors [43]. Consequently, MicroLED chips from different donor substrates must be precisely and rapidly integrated onto a receiving substrate that provides both electrical drive and mechanical support. However, for a display with a resolution of 1920×1080, the traditional pick-and-place method can take several weeks to complete the assembly process. Moreover, for high-definition displays, maintaining an extremely low defect rate is critical. To achieve both high efficiency in MicroLED chip assembly and ensure a very high yield rate, the development of mass transfer strategies for MicroLED chips has emerged as a key research focus for numerous research teams and companies globally [44–53].

Figure 2 summarizes the representative mass transfer strategies for MicroLED chips since the inception of MicroLED technology. These strategies cover two main approaches. The first involves pick-and-place techniques that use van der Waals forces, electromagnetic forces, or vacuum suction. The second employs fluidic self-assembly methods powered by gravity, capillary forces, and dielectrophoretic forces. Meeting critical performance metrics including high efficiency, high precision, high yield, and low cost remains challenging. Addressing this issue requires both significant investment and sustained long-term research efforts. In recent years, a significant number of comprehensive and detailed review papers have been published regarding the development history of MicroLED displays. By 2022, Prof. YongAn Huang's group had made remarkable progress in laser-assisted technology and provided an in-depth analysis of mass transfer printing strategies primarily based on laser-assisted techniques [5,32]. Zhu et al. conducted a systematic review of the production process of MicroLED displays, covering mass transfer, detection, and repair technologies [38]. Moreover, Chen et al. reviewed the key integration technologies for MicroLED displays, including transfer integration, bonding integration, and growth integration [17]. Additionally, there are extensive review articles

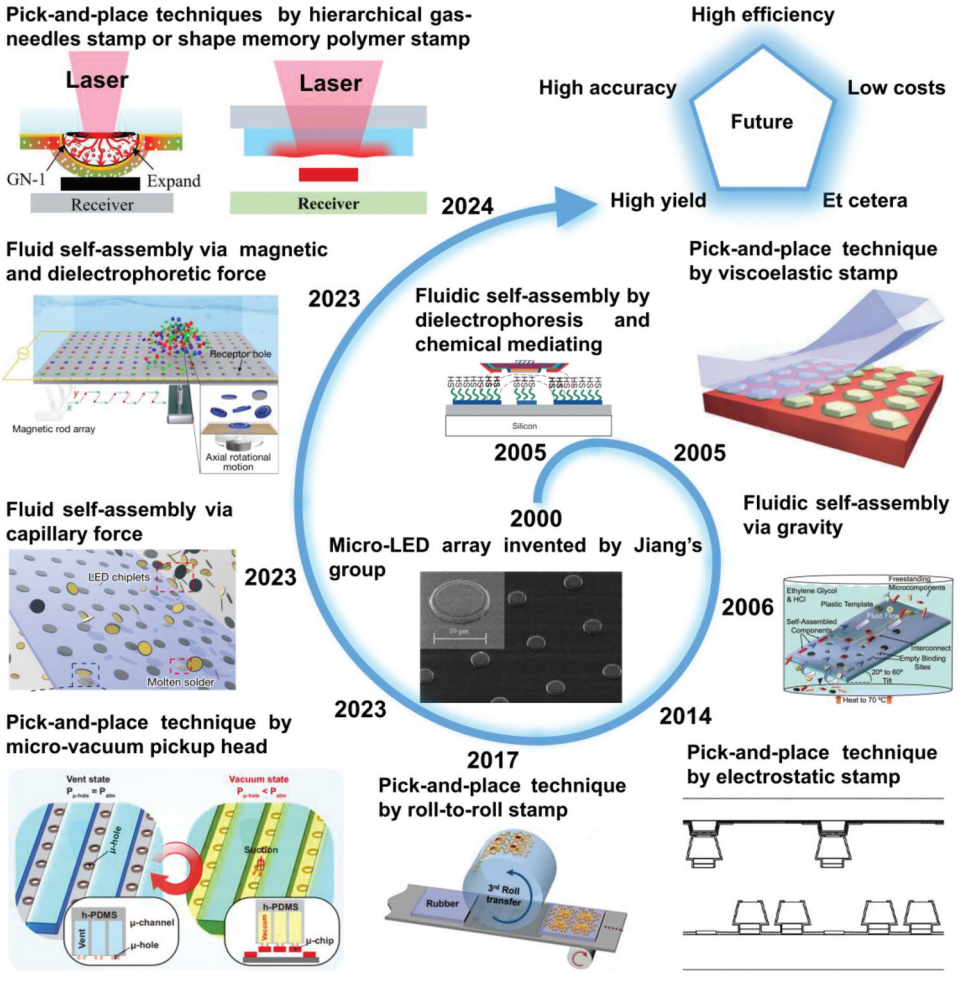

Figure 2. Developmental history and representative achievements in mass transfer strategies for MicroLED chips.

available on quantum dot display technology, full-color display technology, and the overall industrial chain development of MicroLED displays [54–59]. In this review, the focus is on two aspects of mass transfer strategies, namely, pick-and-place techniques and fluidic self-assembly methods. Each strategy is analyzed in detail, discussing the working mechanisms, advantages, and disadvantages based on specific research findings. It is anticipated that this review will facilitate further research on mass transfer strategies for MicroLED chips and contribute to the advancement of the MicroLED display industry.

2. Mass transfer strategies for MicroLED chip assembly

Mass transfer of MicroLED chips typically involves two key processes: releasing the MicroLED chips from the donor substrate and accurately transferring them to a receiving substrate with electrical drive functionality using a temporary transfer medium [60]. In the release process,

a sacrificial layer (e.g. a GaN buffer layer) is introduced on the donor substrate [61–70], allowing the MicroLED chips to be detached via high-energy methods such as laser ablation or chemical etching. The transfer process uses various temporary media including elastic stamps, electrostatic stamps, vacuum stamps, and fluidic systems. Their goal is to precisely position MicroLED chips on designated binding sites [71]. The mass transfer strategy utilizing stamps as transfer media is referred to as the pick-and-place technique, whereas the strategy employing fluids as transfer media is known as the fluidic self-assembly method.

2.1. Pick-and-place techniques

The pick-and-place techniques fundamentally depend on the precise control and switching of adhesion strengths at three critical interfaces: MicroLED chip/donor substrate, transfer stamp/MicroLED chip, and MicroLED chip/receiver substrate. In the pickup phase, the adhesion strength is increased between the transfer stamp and the MicroLED chip. This ensures the chip is reliably lifted from the donor substrate. It also keeps the chip securely held during rapid transfer. In the placement phase, the adhesion strength is reduced between the transfer stamp and the MicroLED chip. This allows quick release of the chip. It also ensures accurate positioning on the receiver substrate. Consequently, various pick-and-place techniques have been developed, leveraging different adhesion mechanisms to achieve parallel regulation of interfacial adhesion [72–87].

2.1.1. Pick-and-place techniques by viscoelastic stamp

The pick-and-place technique utilizing viscoelastic stamps was initially introduced by the research groups of Prof. Rogers and Prof. Yonggang Huang at Northwestern University, U.S.A. [88]. Viscoelastic stamps are typically fabricated using superelastic materials, such as polydimethylsiloxane (PDMS), through a demolding process. During the peeling process, viscoelastic dissipation occurs at the adhesion interface between the viscoelastic stamp and the substrate, as illustrated in Figure 3(a). The viscoelastic stamp is shown under a peeling force $\boldsymbol{F}$ from the contact surface. The separation velocity between the viscoelastic stamp and the MicroLED chip significantly influences the interfacial adhesion force. Specifically, a lower separation speed results in weaker adhesion, while a higher speed leads to stronger adhesion. Consequently, the adhesion force between the viscoelastic stamp and the MicroLED chip can be modulated by adjusting the peeling speed of the stamp during the pick-and-place operation [89,90]. In the steady-state condition, the energy release rate G for crack propagation at the interface can be generally expressed as

$$G = \frac{F}{w} \tag{1}$$

where w is the width of the viscoelastic stamp. The adhesion force is determined by the energy release rate at the adhesion interface and the crack length at the peeling interface.

However, the viscoelastic energy dissipation near the crack tip must be taken into account in the dynamic-state condition. Consequently, the critical energy release rate for the viscoelastic stamp peeling from the contact surface increases monotonically with velocity, as illustrated in Figure 3(b). This relationship follows a general power law and can be expressed as

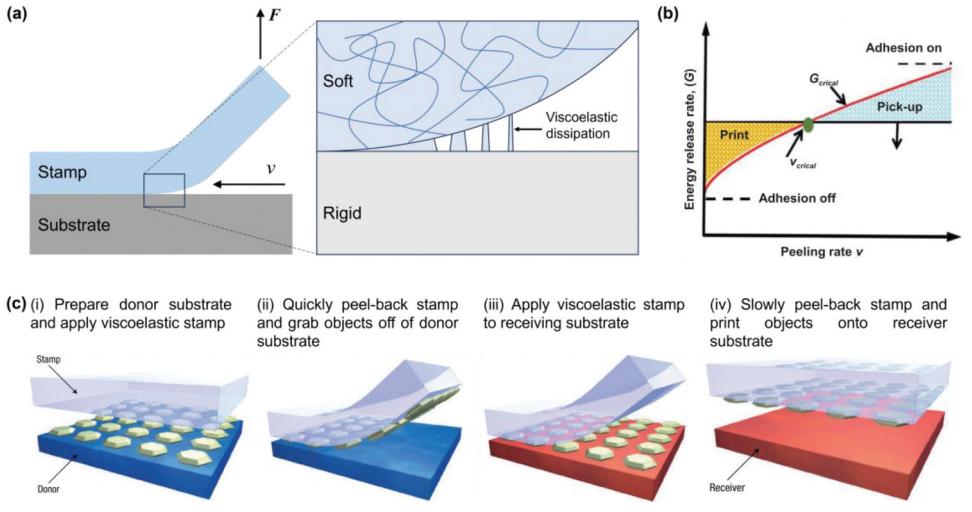

Figure 3. Pick-and-place techniques by viscoelastic stamp. (a) Schematic of the viscoelastic stamp peeled from the contact surface. (b) The relationship of the critical energy release rate for the viscoelastic stamp and the peeling velocity, reproduced with permission from [89]. (c) Pick-and-place operations of the MicroLED chips by a viscoelastic stamp, reproduced with permission from [88].

$$G_c^{stamp/MicroLED}(v) = G_0\left[1 + \left(\frac{v}{v_0}\right)^n\right] \tag{2}$$

where G_0 is the critical energy release rate when the peeling speed approaches zero, v is the peeling speed, v_0 is the reference speed associated with G_0, and n is the scaling parameter. Notably, both the donor substrate, the MicroLED chip, and the receiver substrate exhibit elastic behavior [91]. This suggests that the critical energy release rates at the interfaces between the MicroLED chip and the donor substrate, as well as between the MicroLED chip and the receiver substrate, remain approximately constant. Consequently, the adhesion strengths of these interfaces are nearly independent of the peeling speed. Therefore, there exists a critical peeling speed at which the critical energy release rates at the interfaces between the MicroLED chip/donor substrate and the viscoelastic stamp/MicroLED chip are equal. Similarly, there exists another critical peeling speed at which the critical energy release rates at the interfaces between the MicroLED chip/receiver substrate and the viscoelastic stamp/MicroLED chip are equal. When the peeling speed exceeds the critical peeling speed, the MicroLED chip detaches from the donor substrate. Conversely, when the peeling speed is below the critical peeling speed, the MicroLED chip releases from the viscoelastic stamp and transfers to the receiver substrate. Based on this adhesion force regulation mechanism, the pick-and-place operations of the MicroLED chips can be effectively realized, as illustrated in Figure 3(c).

Compared with flat viscoelastic stamps, stamps featuring a structured contact surface design can dynamically adjust the contact area in response to varying loads, thereby modulating adhesion performance. Utilizing this strategy, the research group of Prof. Rogers and Prof. Yonggang Huang introduced a pyramidal microstructure on the stamp's contact surface [92]. During the pickup of the MicroLED chip, these pyramidal microstructures deform under high loads, resulting in a contact area nearly equivalent to that of

a flat stamp. This allows for rapid peeling of the MicroLED chip from the donor substrate, enhancing the adhesion strength between the stamp and the chip. During MicroLED chip placement on the receiving substrate, the pyramidal microstructures return to their original shape when the load is removed. This recovery reduces the contact area between the stamp and the chip. The stamp is then slowly peeled off from the chip, facilitating its placement on the receiving substrate. Experimental results demonstrate that the range of adhesion modulation achieved by the pyramidal microstructures before and after deformation exceeds three orders of magnitude.

In addition to the structured design of pyramidal microstructures, the group also introduced viscoelastic stamps featuring inclined micropillars, as illustrated in Figure 4(a) [93]. Compared with conventional flat viscoelastic stamps, this inclined micropillar structure introduces a directional dependence on the adhesion strength between the viscoelastic stamp and the MicroLED chip. This characteristic makes the viscoelastic stamp particularly suitable for roller operation mode applications, as depicted in Figure 4(b) [94]. Specifically, as shown in Figure 4(c), during forward rolling, the inclined micropillar structure forms a relatively smaller contact angle with the substrate, whereas during reverse rolling, it forms a relatively larger contact angle [93]. Consequently, the energy release rate during forward rolling is significantly higher than that during reverse rolling, considering the viscoelastic effect.

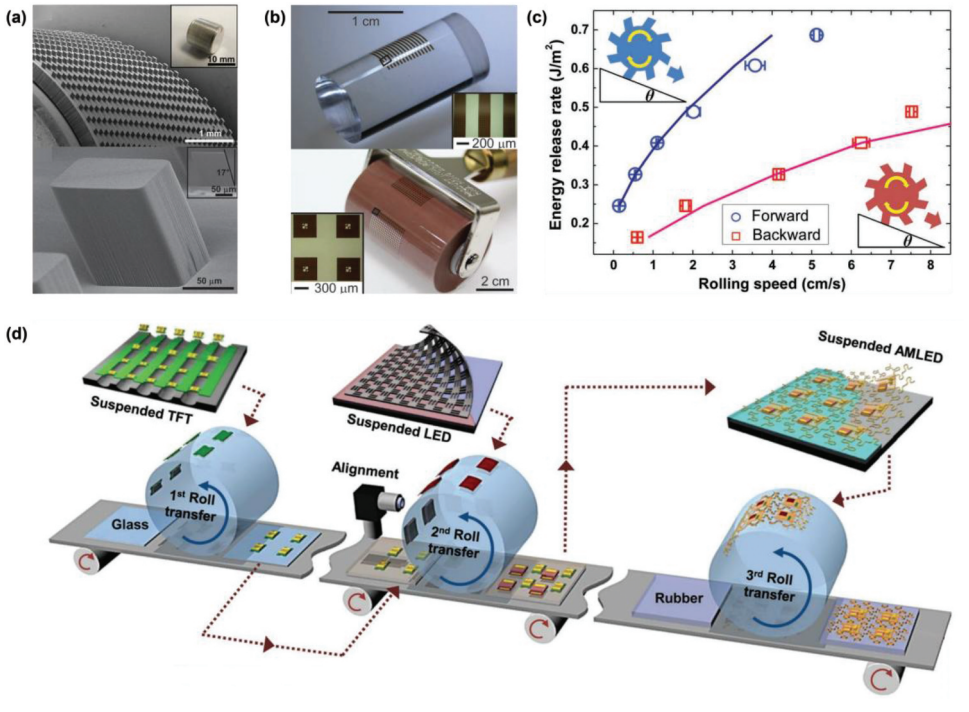

Figure 4. Pick-and-place techniques by structured viscoelastic stamp. (a) Viscoelastic stamps featuring inclined micropillars, reproduced with permission from [93]. (b) Roller-type stamps with inclined micropillar structures, reproduced with permission from [96]. (c) The relationship of the energy release rate for the Roller-type stamps and the peeling velocity during forward and reverse rolling, reproduced with permission from [93]. (d) Roll-to-roll technique utilizing roller-type viscoelastic stamps for MicroLED chip transfer printing, reproduced with permission from [105].

Roller-type stamps have been developed for roll-to-roll transfer techniques owing to their advantages such as lower cost and higher efficiency [95–104]. In 2017, Choi et al. introduced a roll-to-roll technique utilizing roller-type viscoelastic stamps for MicroLED chip transfer printing, as illustrated in Figure 4(d) [105]. During the initial two steps of transfer printing, silicon thin-film transistors, and MicroLED chips were sequentially adhered to the roller stamp by rolling it over a block-type insulated-on-silicon wafer and an AlInGaP wafer, respectively. After completing the pickup operation, the array of silicon thin-film transistors and MicroLED chips on the stamp are transferred onto a stretchable rubber or flexible plastic substrate. This three-step transfer printing process is performed using an automated roll-to-roll transfer system equipped with overlay alignment capabilities, ensuring high stability and reliability. Consequently, the roll-to-roll transfer method demonstrates significant potential for mass transfer printing of MicroLED chips due to its rapid transfer rates, high transfer yields, scalability, stability, and reliability.

The utilization of viscoelastic stamps for transferring quantum dots (QDs) onto MicroLED chips to achieve full-color display represents one of the current research focal points [54,55,58,106–112]. The technologies employed for QD transfer primarily encompass letterpress printing [22], gravure printing [113], sacrificial layer-assisted printing [114], and printing integrated with Langmuir-Blodgett film [115]. Kim et al. proposed the use of a PDMS stamp featuring a tabular structure to pick up QD films from a donor substrate [66]. Owing to the viscoelastic properties of the PDMS stamp, the adhesion between the QD film and the PDMS stamp is highly sensitive to the peeling speed applied. Detaching the PDMS stamp from the donor substrate at a sufficiently high peeling speed ensures robust adhesion of the QD film to the PDMS stamp's surface, as depicted in Figure 5(a). In 2011, Samsung achieved a breakthrough with this technology. They fabricated full-color MicroLED arrays, each with sub-pixel dimensions below 100 μm. These arrays were integrated with a driver backplane, enabling a 4-inch patterned full-color display, as illustrated in Figures 5(b,c). Choi et al. employed a flat PDMS stamp to efficiently collect QDs across an entire surface [113]. Patterned QD films were fabricated through a controlled process. First, low pressure was applied to establish conformal contact between the collected QDs and the substrate grooves. Subsequently, a slow separation step was performed. This sequential method ensured precise adhesion modulation and film patterning. This method enables the fabrication of RGB QD pixels with a resolution of 2460 PPI. In 2022, Meng et al. integrated transfer printing with Langmuir-Blodgett film technology, as shown in Figure 5(d) [115]. QDs were initially dispersed on the water surface and self-assembled into a dense film under the compression induced by a slip stack. Thereafter, a PDMS stamp featuring micro-pillars was utilized to pick up and transfer the QDs onto the target substrate, forming a honeycomb pattern. Finally, the QDs were filled into the honeycomb micro-vias via spin-coating. Through this approach, ultra-high pixel density red and green quantum dot light-emitting devices with a resolution of 25,400 PPI were successfully realized, as shown in Figures 5(e,f).

The pick-and-place technique implemented using viscoelastic stamps modulates interface adhesion by dynamically adjusting the peeling speed in real-time. This method is distinguished by its low cost and high efficiency for transferring MicroLED chips. Nevertheless, there exists an inherent trade-off between peeling speed and transfer printing accuracy. An increase in peeling speed leads to

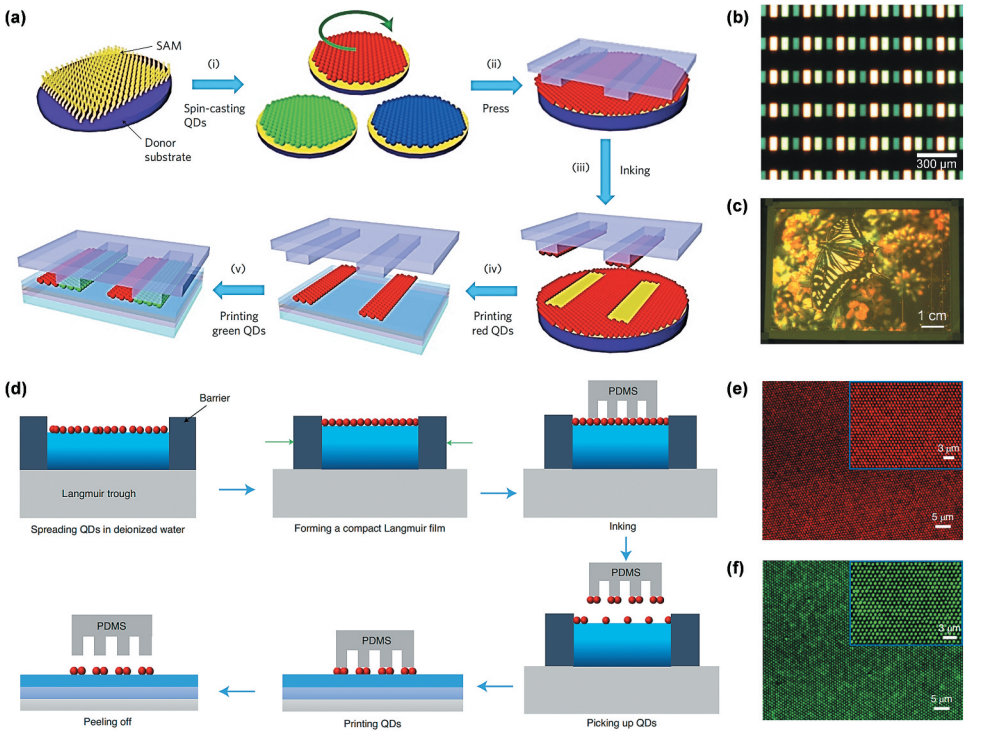

Figure 5. Pick-and-place techniques for QDs. (a) QD transfer by the letterpress printing method, reproduced with permission from [22]. (b) and (c) full-color MicroLED arrays fabricated by Samsung, reproduced with permission from [22]. (d) QD transfer by the printing method integrated with Langmuir-Blodgett film, reproduced with permission from [115]. (e) and (f) red and green quantum dot light-emitting devices, reproduced with permission from [115].

a significant reduction in the placement accuracy of MicroLED chips, thereby posing challenges in fulfilling the stringent requirements of high-resolution displays. Furthermore, the deformation of the viscoelastic stamp results in significant displacement of the MicroLED chip post-transfer, adversely impacting its alignment and bonding accuracy with the receiving substrate.

2.1.2. *Laser-assisted pick-and-place techniques*

Laser serves as a high-energy external light source. By precisely adjusting the parameters of the laser, various physical or chemical reactions can be induced at the interface between the stamp and the MicroLED chip [116–118]. Depending on the extent of the temperature increase, various phenomena such as heating, melting, vaporization, ablation, and plasma formation may be induced. These phenomena serve as the foundation for several laser material processing techniques, as illustrated in Figure 6. Such processes result in alterations to the contact area between the stamp and the MicroLED chip. As discussed in the previous section, modulating adhesion through changes in the contact area is one of the primary strategies for implementing the pick-and-place technique.

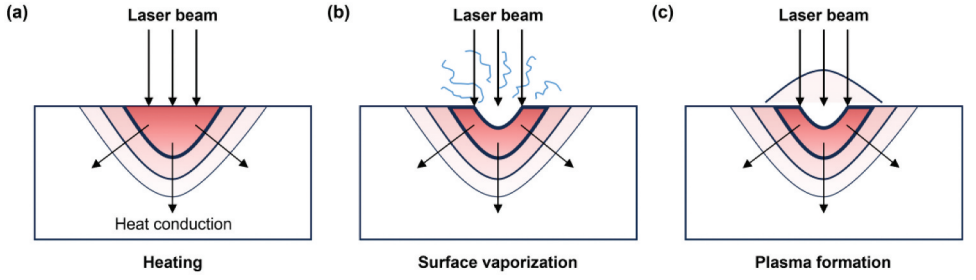

Figure 6. Various laser-material interactions, including heating, surface vaporization, and plasma formation.

2.1.2.1. Thermal expansion mismatch. For viscoelastic stamps fabricated from PDMS, their optical transparency enables a pulsed laser beam to penetrate the stamp and focus precisely at the interface between the stamp and the MicroLED chip. Saeidopourazar et al. reported a pick-and-place technique that exploits the thermal expansion mismatch properties of different materials [119]. As illustrated in Figure 7(a), a viscoelastic stamp holding a MicroLED chip is positioned near the receiving substrate. Subsequently, an infrared pulsed laser beam with a wavelength of 805 nm is directed through the transparent stamp to focus on the adhesion interface. The laser light is absorbed by the MicroLED chip, heating the adhesion interface. Due to the significant difference in the coefficients of thermal expansion between the two materials at the interface, their free expansion is constrained by each other. This thermal expansion mismatch results in bending delamination of the stamp from the MicroLED chip, as depicted in Figure 7(b) [120]. This phenomenon has been validated through high-speed camera observations and theoretical calculations [121–124]. Moreover, this pick-and-place technique is largely independent of the surface characteristics and structure of the receiving substrate, enabling printing on low-adhesion surfaces, curved surfaces, and recessed areas. Consequently, this pick-and-place technique is also referred to as laser-assisted non-contact transfer printing.

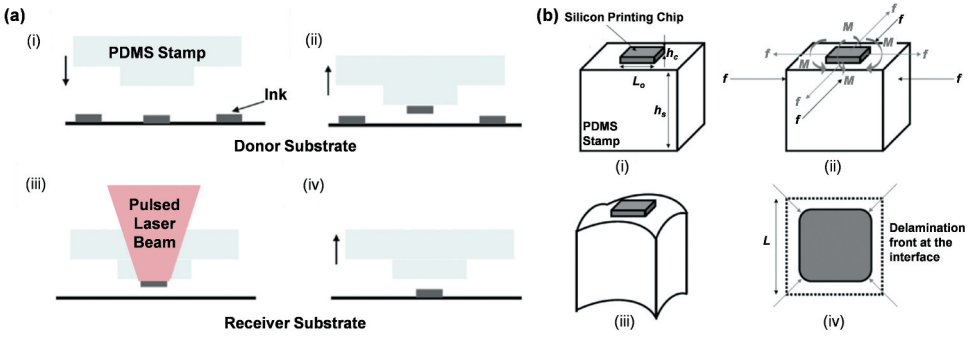

Figure 7. (a) Schematic of the pick-and-place technique based on the thermal expansion mismatch properties of different materials, reproduced with permission from [119]. (b) Theoretical modeling of thermal expansion mismatch, reproduced with permission from [120].

2.1.2.2. Vaporization and ablation. Adding a laser-absorbing layer to the adhesive side of the stamp and utilizing the ablation or vaporization of this layer to detach the MicroLED chip is a widely adopted strategy [125]. This approach, initially introduced in 1986 by Bohandy et al. [126], is known as laser-induced forward transfer (LIFT) [127–129]. Subsequent research has led to the development of numerous pick-and-place techniques based on LIFT, each with notable limitations [130–132]. For instance, high-energy shock waves generated during the ablation or vaporization process may damage the chip, while the rapid detachment of the chip may adversely affect placement accuracy. These issues significantly restrict the practicality of this strategy.

Marinov et al. developed a thermo-mechanical selective laser-assisted transfer method to address the above challenges [133,134]. As illustrated in Figure 8(a), this technique involves adding a dynamic release layer (DRL) consisting of a blistering layer and an adhesive layer to the stamp's adhesion side. When the laser focuses on the DRL, only a localized portion of the blistering layer undergoes ablation, confined within the adhesive layer, as depicted in Figure 8(b). The DRL forms an expanding bubble akin to a soft needle, gently releasing the MicroLED chip from the stamp. The entire release process

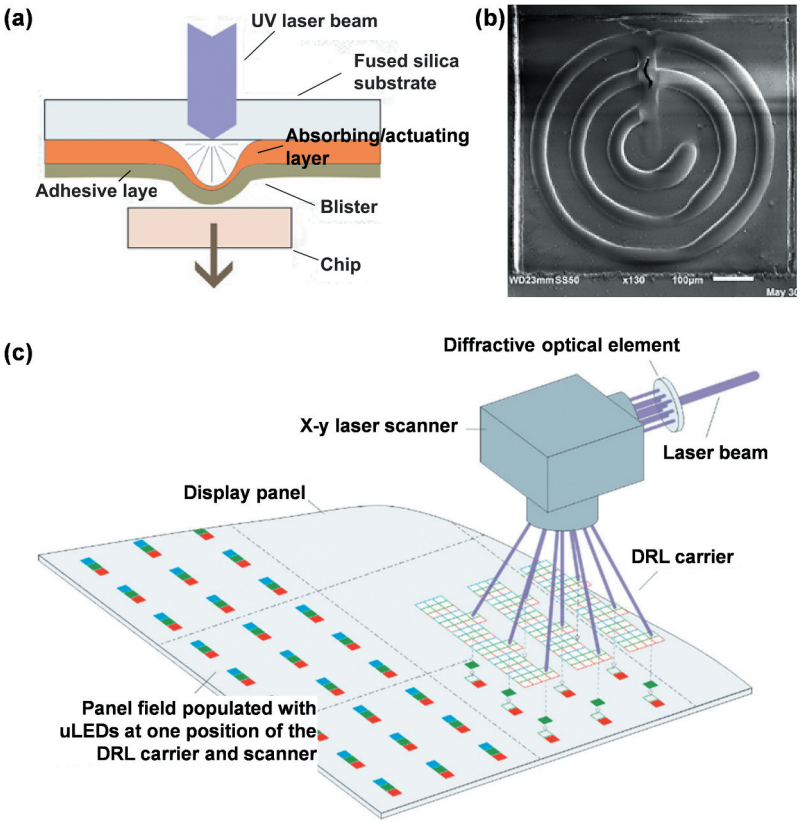

Figure 8. (a) Schematic of dynamic release layer based on thermo-mechanical response, reproduced with permission from [133]. (b) SEM image of the expanding bubble confined within the adhesive layer, reproduced with permission from [133]. (c) Schematic of parallel laser transfer technique, reproduced with permission from [135].

occurs in less than 50 μs, achieving a placement error of merely 1.8 μm. Moreover, advancements in laser technology have enabled the parallel laser transfer technique. This technique facilitates the simultaneous transfer of a large number of MicroLED chips using a single laser pulse, as shown conceptually in Figure 8(c) [135]. However, the irreversible nature of the ablation process prevents stamp reuse, posing a significant challenge for this pick-and-place technique.

2.1.2.3. Thermal expansion. To address the challenges of non-reusability, Luo et al. developed a reusable stamp featuring a microcavity structure [136]. This stamp comprises a microcavity filled with air, a metal layer adhered to the cavity walls, and an adhesive layer with microstructures. Upon laser irradiation, the metal layer absorbs the laser energy, generating significant heat that causes the air within the cavity to rapidly expand. Consequently, the adhesion strength of the stamp transitions from a strong to a weak state, with a difference exceeding three orders of magnitude. However, reducing the geometric size of this ingeniously designed stamp while maintaining high precision remains a significant challenge for this technique.

In 2020, Wang et al. introduced a strategy involving the incorporation of expandable microspheres into the stamp material [137]. By altering the contact area under laser irradiation, they achieved modulation of the adhesion force. Initially, the small size of the expandable microspheres ensures a flat topography on the contact surface, resulting in minimal impact on the stamp's adhesion strength. When stimulated by laser light, these microspheres expand dramatically, inducing layered microstructures on the contact surface and significantly reducing the adhesion strength, as illustrated in Figure 9(a). Figures 9(b,c) depict the surface micromorphology of the stamps at room temperature and high temperature, respectively. The thermally expanding microspheres increased in volume from a diameter of 10 μm to 45 μm without forming any air bubbles. Additionally, the measured surface profile shows the simple yet robust way to actively form visible surface hierarchical microstructures on a shape-conformal stamp through external thermal stimuli (Figure 9(d)). A thin MicroLED chip was positioned on the stamp both before and after heating, clearly demonstrating the significant change in contact area (Figure 9(e)). As shown in Figure 9(f), leveraging the rapid and exceptional adhesion switching capability of this stamp under laser stimulation, a promising transfer technique can be developed. The method integrates a digitally controllable, highly localized laser heating system. It facilitates the programmable and selective transfer printing of MicroLED chips with high precision (Figure 9(g)).

Integrating expanding bubbles with thermally expanding microspheres represents a promising strategy for realizing pick-and-place techniques. In 2023, Chen et al. developed a novel stamp design that integrates expanding bubbles and thermally expanding microspheres. The combined mechanisms form a layered air-needle structure that enables dynamic transitions between non-contact and near-contact operational modes [138]. This stamp utilizes a dual laser system (UV and IR lasers) to achieve a three-step transfer process, as illustrated in Figure 10(a). First, by adjusting the UV laser energy density and pulse accumulation, photo-thermal conversion carbon layers form expanding bubbles on the stamp's contact surface, constituting the first layer of air needles. This initial formation does not cause chip detachment but reduces the distance between the stamp and the receiving substrate. Next, an infrared laser irradiates the structure, causing the expanding bubbles to absorb the laser energy and convert it into heat. As the internal gas warms and expands, it

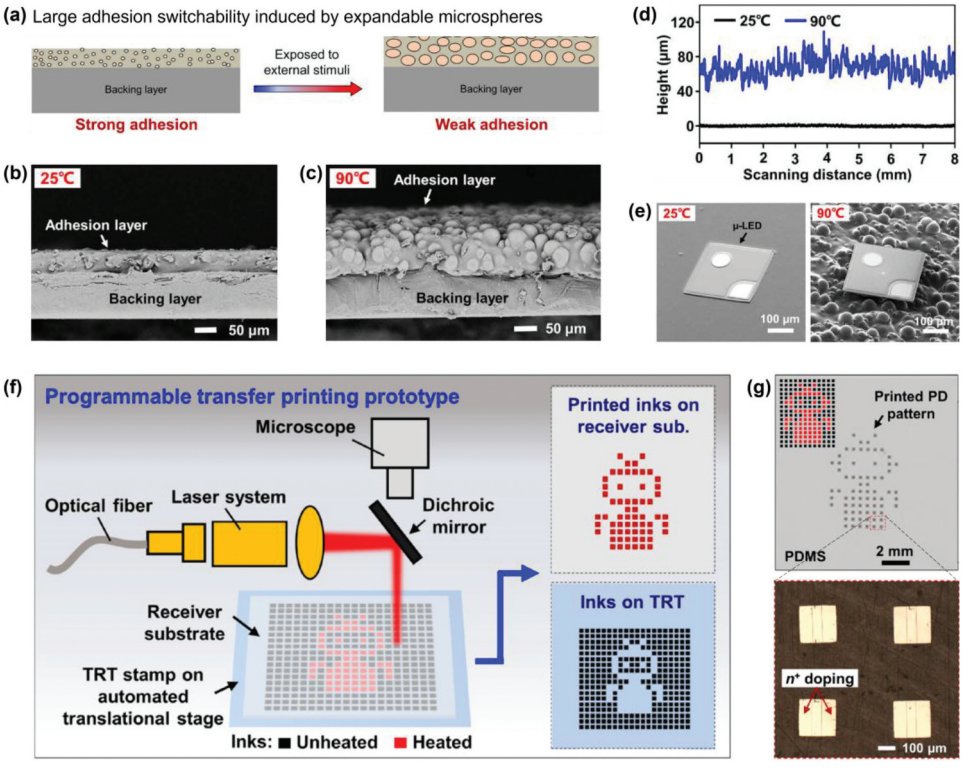

Figure 9. (a) Working mechanism of the thermal expansion stamp, reproduced with permission from [137]. (b) SEM image and (c) corresponding profile of the thermal expansion stamp before and after heating, reproduced with permission from [137]. (d) Profile of the stamp before and after heating, reproduced with permission from [137]. (e) SEM images of the ultrathin MicroLED chip on the stamp before and after heating, reproduced with permission from [137]. (f) Schematic prototype of the laser-assisted programmable pick-and-place technique via automated translational stage, reproduced with permission from [137]. (g) Selectively printed Si chips with a robot-like pattern on PDMS substrate, reproduced with permission from [137].

brings the chip closer to or even into contact with the receiving substrate. Finally, when sufficient heat is conducted through the internal gas, numerous thermally expanding microspheres on the surface of the first layer of air needles expand. The volumetric expansion induces geometric deformation at the stamp-chip interface, and contact area reduction below the adhesion threshold enables spontaneous chip release. The sequential formation of the layered air needles is critical for adhesion switching and preventing thermal damage to the chip. The programmable control of the laser projection system fulfills the requirement for patterned transfer of the chip. As shown in Figure 10(b), a stamp is utilized to pick up the chips from a sapphire substrate and selectively place the chips onto a PDMS substrate. A key advantage of this laser-assisted pick-and-place technique is its proximity printing mode, which can transition from non-contact to contact mode when the initial gap distance between the stamp and the receiving substrate is appropriately set. However, as the authors state in their summary, the dimensions of the thermally expanding microspheres play a crucial role in determining the efficacy of ultrasmall chip transfer.

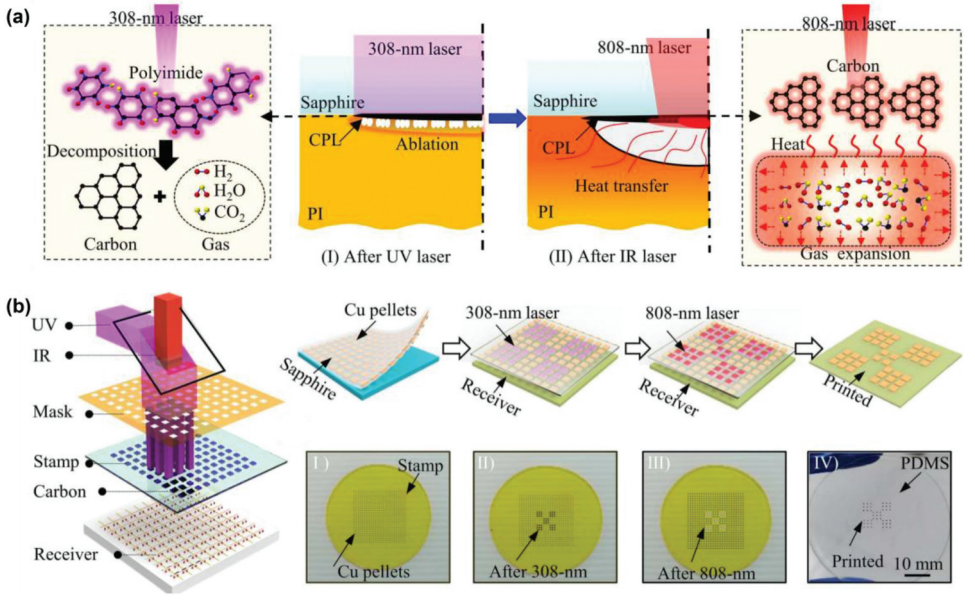

Figure 10. (a) Working mechanism of the layered air-needle stamp, reproduced with permission from [138]. (b) Demonstration of the programmable assembly ability of micro-chips, reproduced with permission from [138].

2.1.2.4. Shape memory polymers. In addition to common viscoelastic materials such as PDMS, Ecoflex, and Dragon Skin, shape memory polymers (SMPs) are frequently utilized in pick-and-place techniques for stamp fabrication [139,140]. SMPs, as a class of smart materials with temporary shape memory, consist of a fixed phase and a reversible phase (Figure 11). The fixed phase retains the original shape of the material regardless of temperature changes, while the reversible phase exhibits temperature-dependent softening and hardening. Below the transition temperature, the molecular chains in the reversible phase remain immobilized, fixing the material's shape. Above this temperature, these chains enter an elastic state, allowing them to deform under external forces or revert to their original configuration due to the influence of the fixed phase. Consequently, SMPs exhibit macroscopic shape recovery behavior.

Based on the mechanism of SMP described above, Eisenhaure et al. proposed a stamp featuring pyramidal microstructures fabricated using SMP [141,142]. Laser heating can

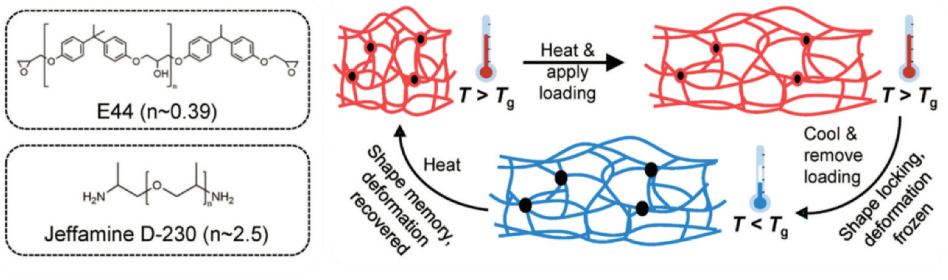

Figure 11. Working mechanism of SMP, reproduced with permission from [144].

dynamically regulate the contact area between the SMP stamp and the chip, thereby modulating the adhesion force. The pick-and-place technique operation process utilizing this stamp is illustrated in Figure 12(a). Initially, the heated SMP stamp contacts the chip while in its elastic state, resulting in a larger contact area. Subsequently, upon cooling, the SMP stamp solidifies, allowing for easy pickup of the chip. As the SMP stamp moves over the receiving substrate, a laser pulse selectively irradiates the interface between the chip and the SMP stamp at the point of release. The laser-induced heating causes the SMP stamp to revert to its original pyramidal shape, reducing the contact area and enabling precise placement of the chip onto the receiving substrate. This strategy leverages the thermally induced shape change of an array of microstructured SMP stamps. Experimental measurements of the relationship between laser power and thermal response demonstrate that carbon black-doped SMP facilitates rapid and localized heat transfer, as shown in Figure 12(b). Furthermore, the gold-coated chips can almost completely reflect the IR laser, preventing damage to the chip and enabling selective placement on a flexible PDMS receiving substrate, as depicted in Figure 12(c).

In addition to transferring chips with flat surfaces, SMP stamps also facilitate the transfer of chips featuring microstructures on their surfaces. Under laser heating, the elastic modulus of SMP can decrease significantly from 3 GPa to 2 MPa. When subjected to a load, the SMP stamp can achieve intimate contact with complex chip surfaces. By maintaining the load and removing laser heating, the SMP stamp becomes rigid and securely adheres to the complex chip surface, providing robust

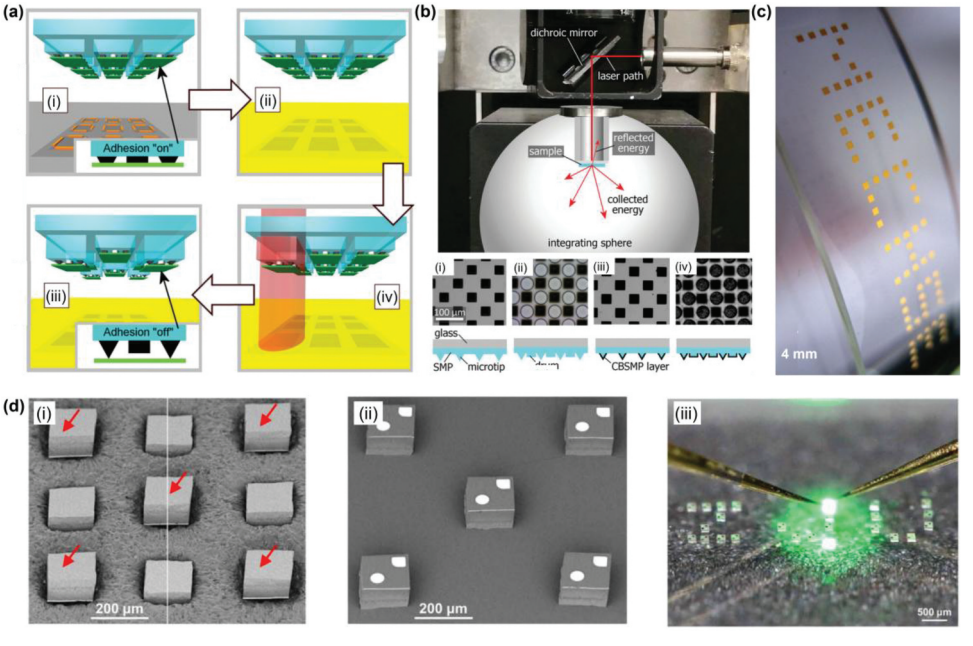

Figure 12. (a) Pick-and-place process by the SMP stamp featuring pyramidal microstructures, reproduced with permission from [141]. (b) Experimental measurements of the relationship between laser power and thermal response, reproduced with permission from [141]. (c) Gold-coated chips placed on a flexible PDMS receiving substrate, reproduced with permission from [141]. (d) Selective printing of MicroLED chips using a programmable laser heating device, reproduced with permission from [143].

pick-up force. To release the chip, laser heating is reapplied, causing the SMP stamp to revert to its initial state. In 2020, Linghu et al. utilized this mechanism of the SMP stamp for selective printing of MicroLED chips using a programmable laser heating device [143]. As illustrated in Figure 12(d), five MicroLED chips were selectively released from a 3×3array. Post-transfer printing, the MicroLED chips demonstrated normal operating performance. In 2023, Linghu et al. elucidated the working principle and developed a mechanics model for the SMP stamp that successfully addressed the adhesion paradox and switchability conflict on rough surfaces [144]. Specifically, their work enabled both enhanced adhesion and facile separation on rough surfaces.

Recently, Li et al. leveraged the remarkable adhesion modulation capabilities of SMP stamps to investigate pick-and-place techniques for LED chips, as illustrated in Figure 13(a) [145]. The experimental results demonstrated that SMP stamps with superior adhesion enhancement properties enabled successful pickup from adhesive substrates such as blue tapes commonly used in industry while leaving the unheated portions of the blue tape unaffected. This strategy was effective for both MiniLED chips of larger sizes (Figure 13(b)) and MicroLED chips of smaller sizes (Figure 13(c)). To systematically evaluate the speed and accuracy of laser heating for non-contact printing of MicroLED chips, they developed a detection platform comprising a displacement control system, an integrated laser and monitoring system, and a pressure detection system. The displacement deviation was as low as 1.4 μm, representing only 2.3% of the chip size, and the placement process could be completed within 3 ms. This high-precision performance facilitated the precise placement of MicroLED chip arrays in the gaps between MiniLED chips, as shown in Figure 13(d).

Laser-assisted pick-and-place technology, driven by programmable control systems, facilitates the selective transfer of MicroLED chips with high precision and efficiency. Nevertheless, the high cost of equipment and the demanding technological requirements represent significant limitations of this approach. The selection of laser wavelength and precise control of energy density are critical factors in achieving successful chip transfer. Typically, lasers within the UV wavelength range (266 nm) possess high photon energy, enabling them to decompose the photo-thermal response layer located between the chip and the carrier via interfacial ablation. Rapid modulation of adhesion is achieved by interfacial ablation. In contrast, lasers in the IR wavelength range (808 nm) enable more controllable photothermal conversion, regulating adhesion forces through the thermal expansion effect. Regarding energy density, an excessively low value (less than 1 mJ/cm^2) may result in insufficient interfacial reactions and residue formation on the chip. Conversely, an overly high energy density (more than 5 mJ/cm^2) can induce material carbonization, potentially causing chip fractures or substrate damage. Thus, despite significant advancements in laser-assisted pick-and-place techniques, transfer printing of MicroLED chips remains challenging in achieving the commercial demands for high precision, high throughput, and high transfer efficiency.

2.1.3. Electrostatic and electromagnetic-assisted pick-and-place techniques

Electrostatic-assisted pick-and-place techniques leverage the attractive and repulsive forces of the electrostatic field to achieve transfer printing of MicroLED chips (Figure 14)

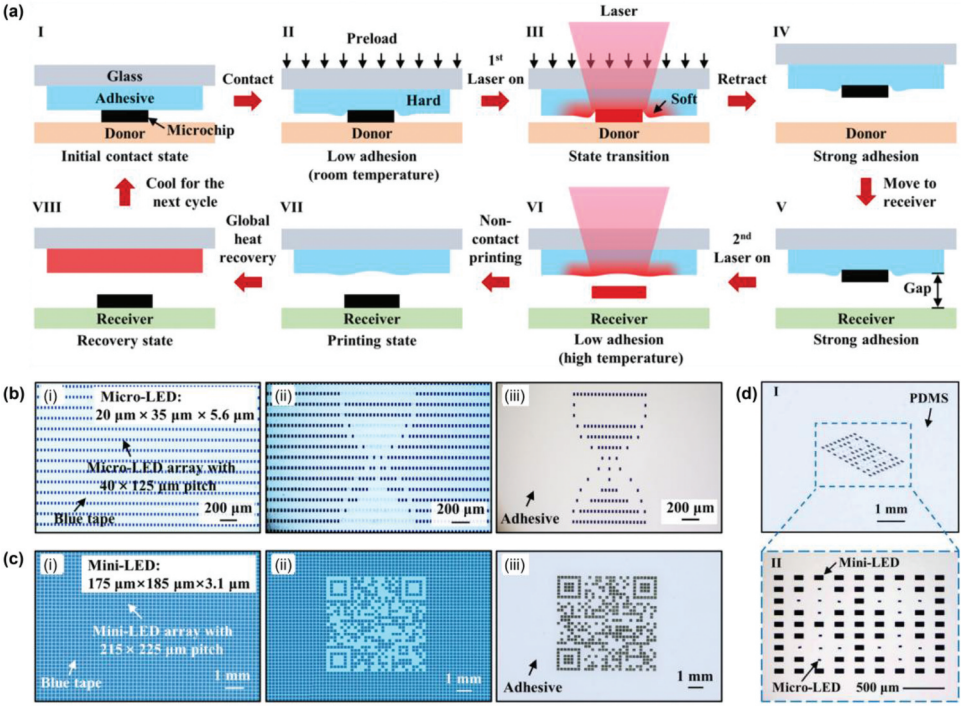

Figure 13. (a) Design of laser-assisted pick-and-place process, reproduced with permission from [145]. (b) MicroLEDsLEDs with a pitch of 40 μm × 125 μm on the blue tape are picked up from the blue tape onto the stamp to form an hourglass pattern, reproduced with permission from [145]. (c) MiniLEDsLEDs with a pitch of 215 μm × 225 μm on the blue tape are picked up from the blue tape onto the stamp to form a 2D code pattern, reproduced with permission from [145]. (d) Deterministic assembly of MicroLEDs and MiniLEDs on PDMS surface, reproduced with permission from [145].

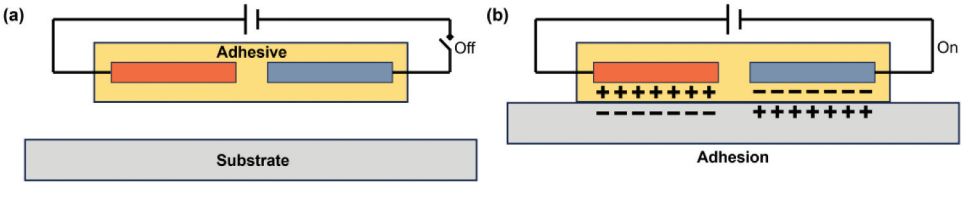

Figure 14. Working mechanism of Electrostatic adhesion.

[146–150]. LuxVue, which was acquired by Apple, has secured several U.S.A. patents in electrostatic-assisted pick-and-place techniques [151–156]. A representative process flow is illustrated in Figure 15(a). Initially, the array of MicroLED chips is immobilized onto a transitional substrate via a primary bonding layer. Next, an electrostatic stamp array, composed of an electrode layer and a dielectric layer, is positioned over the MicroLED chips. Upon applying voltage to the electrostatic stamp array, an attractive electrostatic force is generated between the stamps and the MicroLED chips, enabling each stamp to pick up one MicroLED chip. Subsequently, the electrostatic stamp array, now carrying the MicroLED chips, is transferred to the receiving substrate where the MicroLED chips are

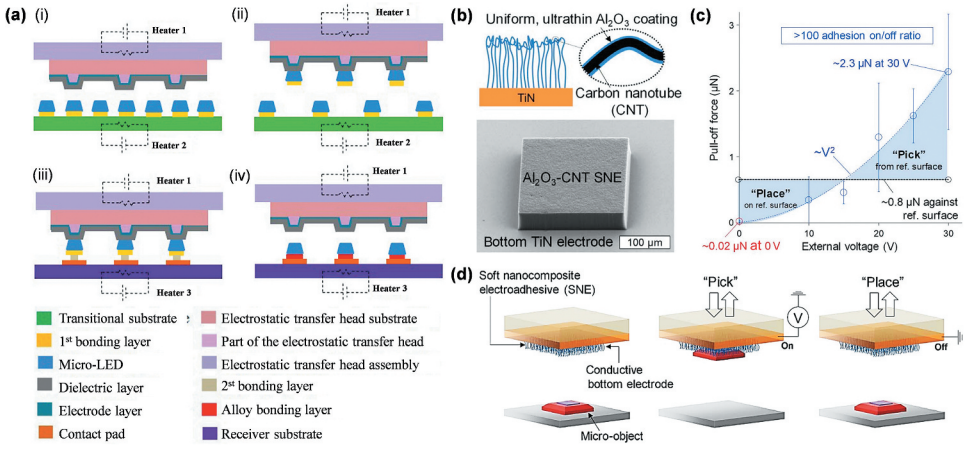

Figure 15. (a) Representative process of electrostatic-assisted pick-and-place techniques, reproduced with permission from [35]. (b) SNE stamp composed of Al_2O_3-coated multi-walled carbon nanotubes, reproduced with permission from [157]. (c) Curve of the pull-off force vs external voltage, reproduced with permission from [157]. (d) Operational workflow of the pick-and-place technique based on SNE stamp, reproduced with permission from [157].

bonded. Finally, the electrostatic stamp array is separated from the MicroLED chips by deactivating the voltage source, altering the AC voltage, or grounding the voltage source to induce electrostatic repulsion.

In 2019, Kim et al. developed a soft nanocomposite electrically-networked (SNE) stamp composed of Al_2O_3-coated multi-walled carbon nanotubes, as illustrated in Figure 15(b) [157]. Upon application of an external voltage, the robust electrostatic adhesion generated by the SNE stamp can surpass the adhesion between the MicroLED chip and the donor substrate, thereby facilitating the pickup of the MicroLED chip, as depicted in Figure 15(c). Once the voltage is removed, the adhesion force of the SNE stamp rapidly diminishes to a negligible level due to its dry adhesive properties, allowing for the easy release of the MicroLED chip. The operational workflow of the pick-and-place technique based on the SNE stamp is presented in Figure 15(d). However, large-scale fabrication of SNE stamps remains challenging, which restricts their broader application. Moreover, excessive static electricity may pose a risk of damaging the MicroLED chip, potentially leading to the failure of light-emitting pixels.

Compared to electrostatic-assisted pick-and-place techniques, electromagnetic-assisted pick-and-place techniques necessitate the incorporation of an additional magnetically sensitive layer within the MicroLED chips to facilitate adhesion with the electromagnetic stamp. A typical process flow for transferring MicroLED chips using electromagnetic stamps is detailed in a patent from the Industrial Technology Research Institute, as illustrated in Figure 16 [158]. Initially, a laser stripping method transfers an array of MicroLED chips onto a temporary substrate featuring an adhesion layer. Subsequently, an electromagnetic stamp array, controlled by an electrical signal, selectively picks up MicroLED chips coated with a sacrificial organic layer from the temporary substrate. Upon removal of the adhesion layer, an attractive force generated between the electromagnetic stamp and the magnetic layer on the MicroLED chip facilitates separation from the temporary substrate. To enhance

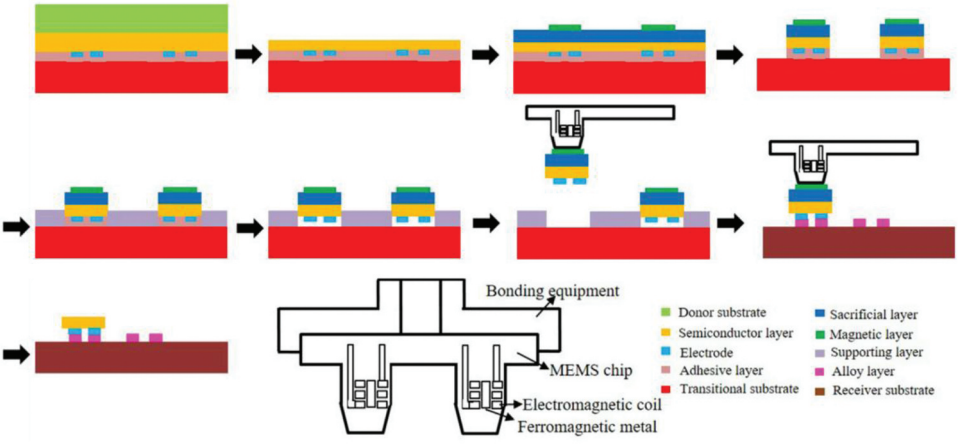

Figure 16. Typical process flow for transferring MicroLED chips using electromagnetic stamps, reproduced with permission from [35].

interaction with the electromagnetic stamp, a magnetic layer composed of Ni, nickel-iron alloy, or other ferromagnetic metals is deposited over the sacrificial layer. The transferred chips are then heated by a heater unit to form a metal alloy layer with the receiving substrate, and the MicroLED chip array is released from the electromagnetic stamp array via the repulsive force generated by the electromagnetic stamp. In electromagnetic transfer techniques, the uniformity of the magnetic material significantly influences the accuracy and consistency of the pick-and-place process.

2.1.4. Pick-and-place techniques by vacuum pickup head

The vacuum-assisted pick-and-place techniques utilize physical adsorption induced by air pressure differences to achieve chip transfer printing [159,160]. During the pickup process, the thimble beneath the chip is actuated upward to disrupt approximately 80% of the adhesion interface between the chip and the blue tape. Subsequently, the vacuum pickup head applies negative pressure to lift the chip, as illustrated in Figure 17(a) [161]. However, this separation process can easily fail due to chip breakage or incomplete detachment from the blue tape [162]. Particularly, as chips become thinner and lighter, the incidence of failure during this process has significantly increased. In 2006, Cheng et al. conducted a comprehensive numerical and analytical study on the peeling behavior of chips from adhesive layers and the shear stress [163]. They concluded that the dimensions of the chip and Young's modulus of the adhesive layer are critical factors influencing the success rate of chip peeling from blue tape. Lin et al. employed the finite element method to examine the impact of key process parameters, such as thimble lifting speed, vacuum pressure, and thimble radius, on the peeling process, aiming to minimize chip breakage.

In 2015, Liu et al. conducted a comprehensive investigation into the competitive fracture behavior of chips during the transfer process [164]. Figure 17(b) illustrates a schematic and localized enlargement of the chip being peeled off from the blue tape. Figure 17(c) outlines the four stages of chip transfer: initial contact between the thimble and the blue tape, lifting of the thimble to strip the chip, pickup of the chip, and

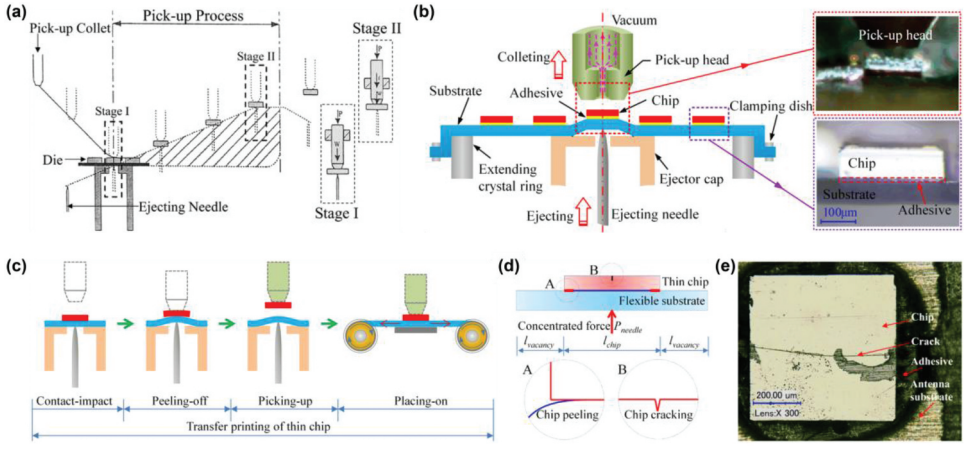

Figure 17. (a) Pickup process by vacuum pickup head, reproduced with permission from [161]. (b) Schematic and localized enlargement of the chip being peeled off from the blue tape by vacuum pickup head, reproduced with permission from [164]. (c) Four stages of chip transfer from the blue tape by vacuum pickup head, reproduced with permission from [164]. (d) Schematic diagram of competing crack paths, reproduced with permission from [164]. (e) Image of a crack propagating through a chip, reproduced with permission from [164].

placement of the chip onto a roll-to-roll receiving substrate. The peeling and cracking of the chip can be considered as two competing fracture mechanisms, namely interface peeling and chip cracking. Figure 17(d) presents a schematic diagram proposed by Liu et al., depicting competing crack paths, where region A represents successful peeling, and region B represents chip cracking. Meanwhile, Figure 17(e) provides a physical image of a crack propagating through a chip, leading to its fracture.

In 2023, Park et al. introduced a micro-vacuum assisted selective transfer (μVAST) strategy for the transfer printing of MicroLED chips from a donor wafer to a receiver substrate using microvacuum force [165]. The fundamental concept is illustrated in Figure 18(a). The pick-and-place device comprises a rigid PDMS substrate with micro-channels and a glass substrate featuring microholes, as depicted in the cross-sectional view in Figure 18(b). During the pick-and-place operation, the pressure within the microchannels of the PDMS substrate transitions from an atmospheric state to a vacuum state by adjusting the pressure. This change generates suction at each microhole in the glass substrate, effectively detaching the MicroLED chips from the donor wafer. For the release process, the suction is promptly terminated by venting the air, allowing the chips to be precisely printed onto the receiving substrate. The vacuum adsorption force is sufficiently strong to sever the u-bridge connecting the chip to the donor substrate without requiring mechanical lifting, thereby significantly reducing the risk of chip damage. The adhesion force test results are presented in Figure 18(c), demonstrating that μVAST achieves an adhesion switching ratio of 3.364×10^6, which is three orders of magnitude higher than other transfer methods. Figure 18(d) showcases the heterogeneous integration of thin-film microchips achieved through μVAST, where chips of varying sizes and thicknesses are assembled on the same substrate in a diagonal configuration.

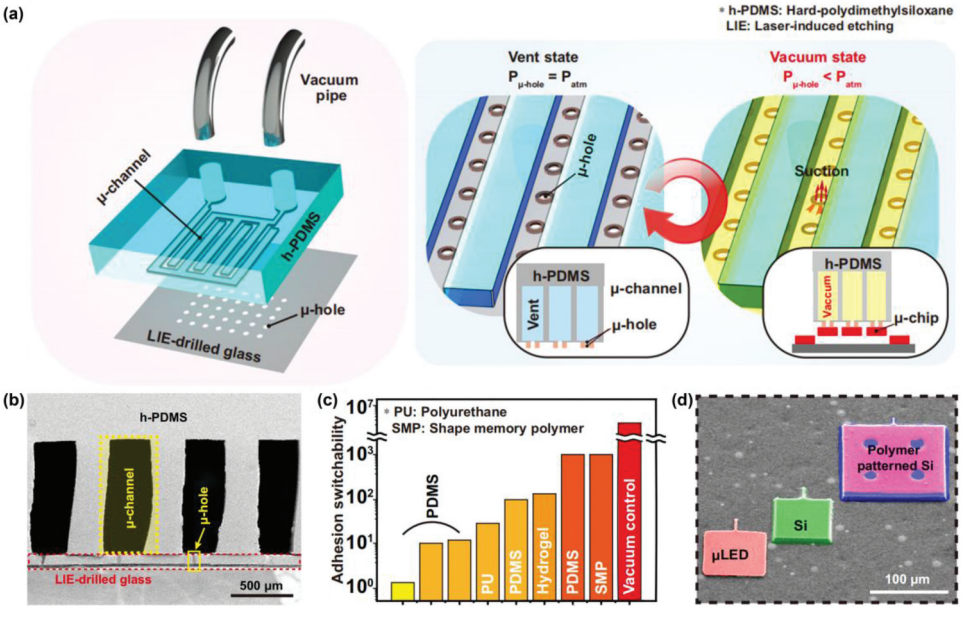

Figure 18. (a) Schematic of μVAST strategy, reproduced with permission from [165]. (b) SEM of the cross-sectional view for the μVAST device, reproduced with permission from [165]. (c) Comparison of adhesion switchability of μVAST with other strategies, reproduced with permission from [165]. (d) Heterogeneous integration of thin-film microchips achieved through μVAST, reproduced with permission from [165].

Vacuum-assisted pick-and-place techniques represent one of the most widely adopted methods for MicroLED chip transfer. However, the microhole and microchannel structures within the pickup device pose a risk of clogging, necessitating routine inspection and maintenance.

2.2. Fluidic self-assembly methods

Fluidic self-assembly represents an innovative and scalable strategy for the mass transfer of MicroLED chips, distinct from traditional pick-and-place techniques [166]. By suspending a large number of MicroLED chips in a fluidic medium, these chips can be precisely guided to predetermined positions through the combined effects of gravity, capillary forces [167], dielectrophoretic force, and other driving forces [168]. Importantly, fluidic self-assembly is not constrained by the size of the MicroLED chips and the precision limitations of machinery. Consequently, this method holds significant potential to surpass pick-and-place techniques, addressing the inherent trade-off between throughput capacity and packaging precision.

2.2.1. Fluid self-assembly via gravity

The gravity-driven fluidic self-assembly strategy leverages the geometric characteristics of the chips and the precisely engineered microholes on the receiving substrate. MicroLED chips suspended in the fluid medium randomly settle into corresponding microholes

under gravitational influence, while excess chips sediment at the bottom of the container for subsequent reuse [169,170]. Yeh and Smith pioneered the investigation of GaAs-LED chip self-assembly on silicon substrates using a combination of fluid transport and shape matching in 1994 (Figure 19(a)) [169]. They designed an inverted trapezoidal structure to facilitate the insertion of the narrower end of the chips into the matched holes, with unmatched chips being washed away by the fluid. Post-assembly, the silicon substrate is removed from the fluid and dried. However, capillary forces during fluid evaporation can dislodge some successfully assembled chips, limiting the highest transfer yield to approximately 70%.

In 2017, eLux refined the strategy initially proposed by Yeh and Smith based on their fluidic self-assembly patent (Figure 19b) [171,172]. The enhancements primarily involved redesigning the structure of the MicroLED chips and the microholes on the substrate. Specifically, a representative cylindrical feature was added to the top of the MicroLED chip. During the fluidic self-assembly process, when the cylindrical end is inserted face down into a microhole, the tilt of the MicroLED chip causes the fluidic drag force to rotate the chip into its correct orientation. If an inverted MicroLED chip flips over but does not align properly, it may be ejected from the current microhole and captured by the subsequent microhole. This improved method achieves yields exceeding 99.9%.

Stauth and Parviz introduced a complementary shape recognition approach for chip self-assembly in 2006 [173]. As illustrated in Figure 19(a,c), a specially designed receiving substrate is positioned at a specific angle within a fluidic container. Under gravitational force, the chips slide downward along the substrate surface. Within 25 minutes of self-assembly, up to 10,000 chips can be assembled, achieving transfer yields exceeding 97% (Figure 19(d)).

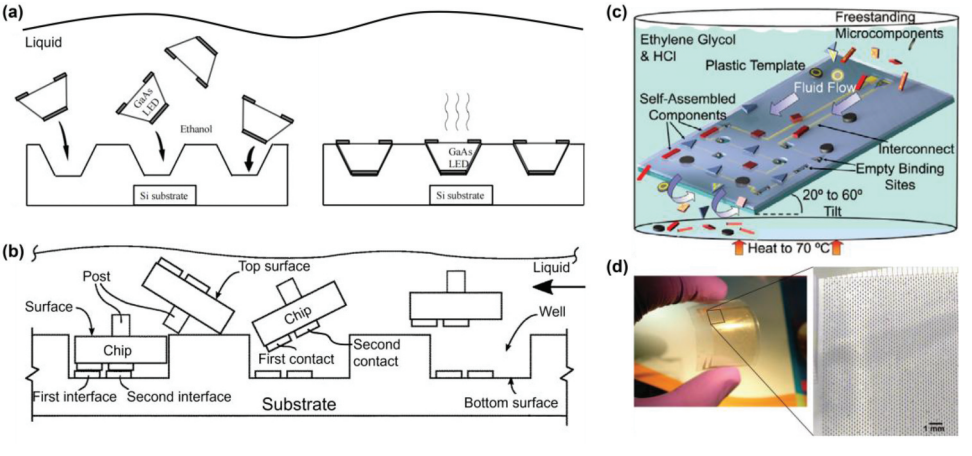

Figure 19. Fluidic self-assembly methods via gravity. (a) GaAsAs-LED chip self-assembly on silicon substrates, reproduced with permission from [169]. (b) MicroLEDoLED chips with a representative cylindrical feature self-assembly on silicon substrates, reproduced with permission from [171]. (c) Schematic diagram of complementary shape recognition approach for chip self-assembly, reproduced with permission from [173]. (d) Self-assembled Micrundefined chip array, reproduced with permission from [173].

2.2.2. Fluid self-assembly via capillary force

Compared to gravity-driven strategies, the capillary force-driven fluidic self-assembly method eliminates the need to consider the shape of the chip. Furthermore, the miniaturized design of the chip enhances the effectiveness of capillary forces. Typically, a liquid or molten solder serves as the connecting medium at the interface between the chip and the receiving substrate, facilitating self-assembly under the influence of surface tension [174,175]. In 2001, Srinivasan et al. utilized water as the connecting medium to drive the capillary force-induced self-assembly of micromachined silicon parts onto silicon and quartz substrates [176,177]. Building on this mechanism, Morris and Parviz in 2007 explored the use of molten solder alloys as a connecting medium for self-assembling chips onto the binding sites of a receiving substrate [178,179]. Initially, a dip-soldering process was performed on the receiving substrate with gold pads etched on its surface. Subsequently, after introducing a large number of chips into the self-assembly solution, the solution was heated and the container rotated. This brought the chips into contact with the molten alloy solder on the receiving substrate, forming a meniscus surface via capillary forces, which guided the chips to their respective binding sites. The mechanism is illustrated in Figure 20(a).

Recently, Lee et al. reported a method to achieve the self-assembly of 19,000 disk-shaped MicroLED chips within 60 seconds by enhancing the viscosity of the self-assembly solution based on the aforementioned mechanism, with a yield exceeding 99.88% [180]. Initially, the sapphire receiving substrate features a patterned circular gold layer at the

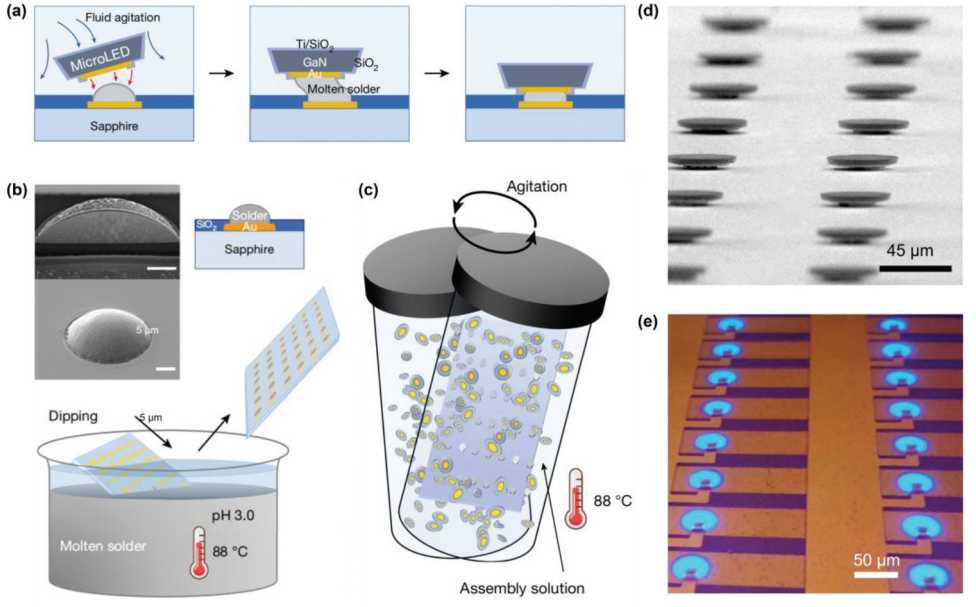

Figure 20. Fluidic self-assembly methods via capillary force. (a) Working mechanism of the fluidic self-assembly methods via capillary forces, reproduced with permission from [180]. (b) Dip-soldering process for the receiving substrate features a patterned circular gold layer, reproduced with permission from [180]. (c) Schematic diagram of the fluidic self-assembly via capillary forces, reproduced with permission from [164]. (d) Image of the self-assembled chip array, reproduced with permission from [180]. (e) Image of blue-light MicroLED lighting panel, reproduced with permission from [180].

binding sites, and a dip-soldering process is employed to form molten solder bumps, as illustrated in Figure 20(b). The receiving substrate and the MicroLED chips, which have a gold-patterned layer on their bottom surfaces, are immersed into the self-assembly solution. Upon heating the self-assembly solution to 88 ℃ and stirring it, contact between the solder bumps and the gold layer is induced, as depicted in Figure 20(c). Figures 20(d,e) present images of the self-assembled chip array and a normally operating blue-light MicroLED lighting panel, respectively.

2.2.3. Fluidic self-assembly via dielectrophoretic force

The dielectrophoretic force is the resultant force acting on a neutral particle in an inhomogeneous electric field, arising from dielectrophoretic polarization. This force induces the translational motion of particles within the electric field and causes varying degrees of electrical dipolarization, aligning the particles along the direction of the applied electric field. Dielectrophoretic force-driven fluidic self-assembly leverages this mechanism to non-contactly manipulate and localize MicroLED chips to designated binding sites. In 2004, O'Riordan et al. introduced a technique for assembling mesoscale objects onto a receiving substrate using programmable electric fields (Figure 21(a)) [181]. The substrate featured a 4×4 array of circular receptor electrodes. By altering the electric field configuration, a MicroLED chip with a diameter of 50 μm could be precisely moved between electrodes, as illustrated in Figure 21(b). In 2005, Lee and Bashir developed a directed self-assembly method that combined dielectrophoretic forces with chemical interactions (Figure 22(a)) [182]. They utilized a functionalized substrate to facilitate Au-S bonding between the chip and the substrate, ensuring stable positioning during solution evaporation, as depicted in Figure 22(b). In 2016, Park et al. demonstrated the successful implementation of electric field-assisted nanorod LED self-assembly technology, utilizing the dielectrophoretic force-driven fluidic self-assembly mechanism [183].

In 2023, Chang et al. introduced a magnetic and dielectrophoresis-assisted self-assembly technique (MDSAT) [184]. This method involves embedding nickel within MicroLED chips, enabling magnetic control, and applying a localized dielectrophoretic force centered on microholes in the receiving substrate. As the

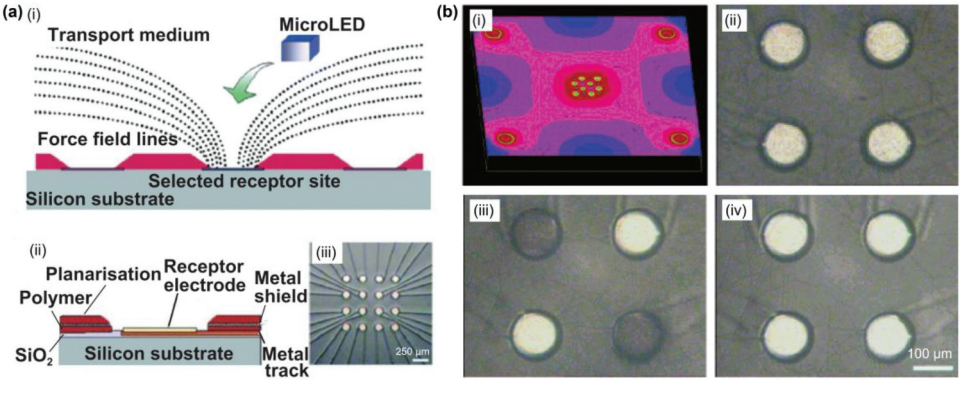

Figure 21. (a) Schematic diagram of fluidic self-assembly via dielectrophoretic force, reproduced with permission from [181]. (b) Simulation and optical micrographs of on-chip electrical field distribution following checker-board addressing, reproduced with permission from [181].

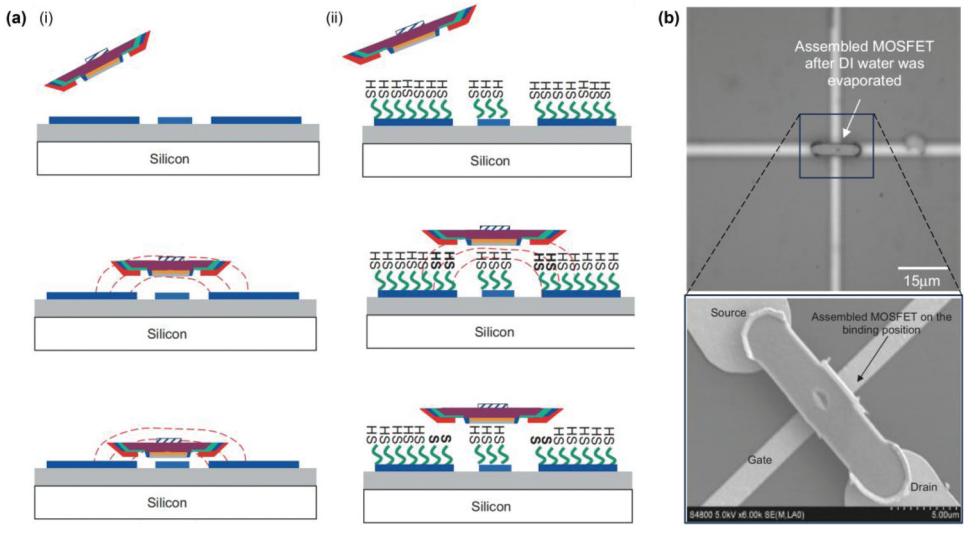

Figure 22. (a) Fluidic self-assembly via dielectrophoretic forces with chemical interactions, reproduced with permission from [182]. (b) SEM images of the assembled device on a binding position, reproduced with permission from [182].

MicroLED chip approaches the microhole, the dielectrophoretic force traps and assembles individual MicroLED chips into the designated microholes. Near the receptor holes, the dielectrophoretic force dominates, while the magnetic force facilitates long-distance transport of the MicroLED chips. Consequently, MicroLED chips can be efficiently captured and assembled at their binding sites. The schematic diagram of the MDSAT process is illustrated in Figure 23(a). Figure 23(b) depicts the distribution of dielectrophoretic and magnetic forces between two receptor holes during assembly. The research results indicate that the transfer yield is influenced by both the applied voltage and the height of the receiving substrate hole. As shown in Figure 23(c), the transfer yield initially increases and subsequently decreases with the rise in voltage. Furthermore, an increase in the hole height promotes the self-healing of shape mismatch defects (Figure 23(d)). This technology enables the simultaneous self-assembly of red, green, and blue MicroLED chips, achieving a transfer yield of up to 99.99% within 15 minutes. Figure 23(e) presents a fabricated 100 mm × 100 mm RGB display panel, comprising 43,200 MicroLED chips. The light-emitting panel exhibits superior emission intensity and brightness uniformity.

Fluid self-assembly is a crucial strategy for the mass transfer of MicroLED chips, offering both low cost and high efficiency. However, the transfer yield remains a key performance metric that requires further enhancement.

3. Conclusions

Mass transfer strategies, which involve the precise transfer of millions or even tens of millions of MicroLED chips from a donor substrate to a receiver substrate, are crucial for

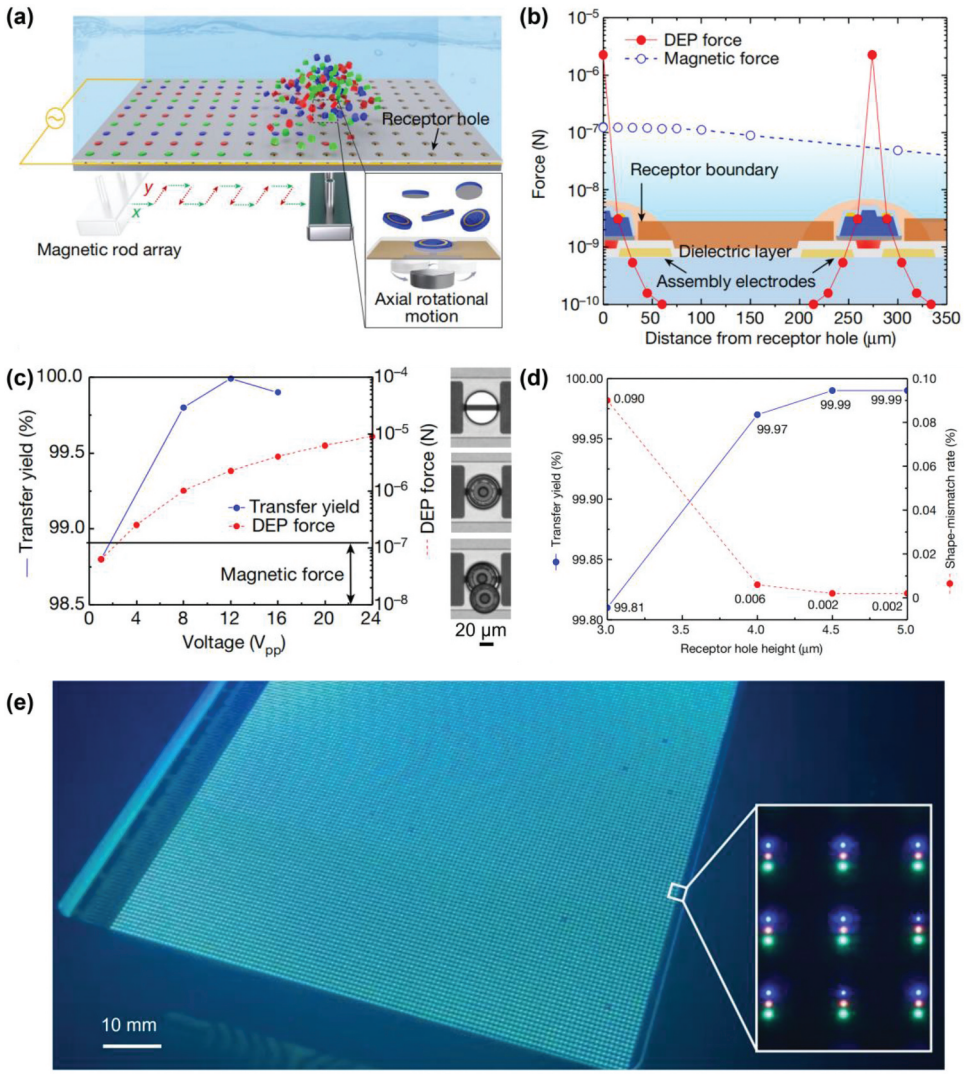

Figure 23. (a) Schematic diagram of fluidic self-assembly via magnetic and dielectrophoretic forces, reproduced with permission from [184]. (b) Distribution of dielectrophoretic and magnetic forces between two receptor holes, reproduced with permission from [184]. (c) Relationship between transfer yield and applied voltage, reproduced with permission from [184]. (d) Relationship between transfer yield and receptor hole height, reproduced with permission from [184]. (e) Photograph of a panel based on RGB MicroLED chips, reproduced with permission from [184].

commercializing MicroLED displays as a next-generation display technology. Over the past two decades, research and development in mass transfer have primarily focused on improving transfer efficiency, placement accuracy, yield of finished products, and reducing manufacturing costs. Table 1 provides a comprehensive comparison of various mass transfer strategies for MicroLED chip assembly, evaluating them based on placement rate, transfer precision, chip size, transfer yield, and cost. Additionally, it systematically summarizes the advantages, disadvantages, and applicable production scenarios of these

Table 1. Comparison of various mass transfer strategies for MicroLED chip assembly.

Strategy	Method	Characteristics	Principle	Placement rate (units/h)	Transfer precision (μm)	Chip size (μm)	Transfer yield (%)	Cost
Pick-and-place	Peeling speed	Flat and elastomer stamp	Viscoelastic dissipation	1 million	1.5	>10	99.99	Low
		Rolling and elastomer stamp	Viscoelastic dissipation	36 million	3	<100	99.9	Low
		Structured and elastomer stamp for QDs	Viscoelastic dissipation	NA	<1	<1	100%	High
	Laser-assisted	Thermal expansion mismatch	Contact area	5 million	NA	100	99.5	Moderate
		Vaporized material	Contact area	500 million	<1	1	99	High
		SMP stamp	Temporary shape memory	0.01 million	NA	35	NA	Moderate
	Electrostatic-assisted	Electrostatic stamp and magnetic coating	Electrostatic force	12 million	0.5	1	99	High
	Electromagnetic-assisted	Electromagnetic stamp	Magnetic force	0.9 million	1	10	99	High
	Vacuum-assisted	Vacuum pickup head	Vacuum pressure	<1 million	4.6	100	98.06	Moderate
Fluidic self-assembly	Shape matching	Fluid media	Gravity	0.024 million	NA	100	97	Low
	Capillary force	Dip-soldering	Surface tension	>1 million	NA	45	99.88	Low
	Dielectrophoretic force	Electric field	Dielectrophoretic polarization	<1 million	0.3	<100	99.99	High

Table 1. (Continued.)

Strategy	Advantage	Disadvantage	Applicable scene
Pick-and-place	Low cost	Low throughput and low efficiency	Limited scale production
	Low cost, high throughput and high efficiency	Direct contact and easily damaged chips	High volume production
	High resolution and multi-color	Low throughput and small pringting area	High resolution device manufacturing
	High efficiency	Difficulty of thermal stress control	Chip stripping on sapphire substrates
	High efficiency and high precision	Material durability	High Resolution Displays
	High stability and low demands on surface flatness	Low efficiency	MicroLED chip integration with complex surfaces
	High precision and ultra-small chip	High process sensitivity and damage to chips	Small size and high value products
	High precision and stability	High material costs and high demands on magnetic field uniformity	Ultra-high precision MicroLED display
	High automation and process maturity	Size limitation cannot be smaller than 50 μm	Low- and mid-range consumer electronics
Fluidic self-assembly	Components can be recycled	Low transfer yield and complex design	Chips in different shapes and sizes
	Self-alignment and high efficiency	Stability of joints and excess contact	Single color LED display
	High transfer precison and multi-material compatible	High cost and process complexity	Small size and high value products

strategies. Among these, pick-and-place techniques, particularly those assisted by lasers, have achieved sub-micron placement accuracy and are considered core technologies for high-precision mass transfer. In contrast, fluidic self-assembly methods offer a high-performance cost ratio for large-scale production of low-resolution displays due to their low-cost and high-efficiency advantages, but they are limited by lower accuracy and yield.

In recent years, as MicroLED display technology has progressively entered the mainstream of the consumer electronics industry, mass transfer strategies, a critical bottleneck for its industrialization, are experiencing multidimensional technological innovation and cross-domain integration. The emergence of mixed strategies, such as pick-and-place techniques utilizing laser-induced viscoelastic stamps and fluidic self-assembly methods driven by magnetic and dielectrophoretic forces, is further transcending the physical limitations of traditional transfer technologies by leveraging the flexibility and precision of non-contact operations.

In future research, the development of mass transfer strategies may focus on the following key areas.

3.1. Improvements in stamp materials

Development of composite stamp materials based on photo/thermally responsive hydrogels. By synergizing the laser-driven adhesion layer (PDMS) with the phase-change layer (hydrogel), an on-demand adhesion and release function for micron-scale chips is achieved. This enhances transfer precision to the submicron level. Furthermore, the density of the hydrogel crosslinking network and nanoparticle doping (e.g. silicon carbide) can be optimized to enhance shear strength while preserving high flexibility. This minimizes chip damage caused by stress concentration during the transfer process. In terms of cost reduction, self-healing shape memory polymers can be developed via dynamic covalent bonding or supramolecular network design.

3.2. Improvement in process technologies

The efficiency and precision of mass transfer printing may be achieved through the development of advanced processes and technologies. For instance, a high-throughput mechanical structure based on roller transfer, in conjunction with fluidic self-assembly technology, enables chip self-alignment, effectively addressing the heterogeneous material compatibility issue in MicroLED chip manufacturing. Moreover, the bipolar electrostatic transfer head can be synergistically combined with electromagnetic adhesion technology to improve the compatibility between flexible substrates and rigid chips, achieving a transfer yield exceeding 99.999%.

3.3. Improvement in intelligent manufacturing

Combining artificial intelligence with the mass transfer strategy enables the establishment of a dynamic optimization model. This model analyzes in real-time the relationships among parameters such as laser power, transfer speed, transfer yield, and accuracy. Artificial intelligence-driven robots can perform fully automatic calibration of transfer equipment, for instance, by achieving high-precision alignment of chips via

a vision positioning system. Furthermore, a deep learning-based visual inspection system is capable of identifying defects such as cracks or offsets in micron-sized chips and adjusting process parameters in real-time through feedback control mechanisms.

In summary, this paper reviews a variety of mass transfer strategies that have been proposed since the inception of MicroLED chips. However, achieving large-area and high-throughput transfer remains a significant challenge that hinders the commercialization of MicroLED chips. With the cross-integration of multiple disciplines, an increasing number of mass transfer strategies are demonstrating substantial potential for practical application. Looking ahead, the widespread adoption and application of MicroLED display technology will become increasingly prevalent. Consequently, research into mass transfer strategies for MicroLED chips is expected to remain a vibrant area of investigation.

Disclosure statement

No potential conflict of interest was reported by the author(s).

Funding

The authors would like to express their sincere thanks to the financial support from the Research Institute for Advanced Manufacturing (RIAM) of The Hong Kong Polytechnic University (project Nos. 1-CD9F and 1-CDK3), the Research Grants Council (RGC) of Hong Kong (project Nos. 25200424 and 15206223), the Basic and Applied Basic Research Foundation of GuangDong (project No.2023A1515110709), and the Startup fund (project No.1-BE9L) of the Hong Kong Polytechnic University. Jinsheng Zhao would like to extend his sincere gratitude for the financial support from the project (PolyU Distinguished Postdoctoral Fellowship Scheme 2024) (4-45-35-YWEC).

References

[1] Wu T, Sher C-W, Lin Y, et al. Mini-LED and Micro-LED: promising candidates for the next generation display technology. Appl Sci. 2018;8(9):1557. doi: 10.3390/app8091557
[2] Miao WC, Hsiao FH, Sheng Y, et al. Microdisplays: Mini-LED, Micro-OLED, and Micro-LED. Adv Optical Mater. 2023;12(7). doi: 10.1002/adom.202300112
[3] Virey E. Are MicroLEDs really the next display revolution? Inf Disp. 2018;34(3):22. doi: 10.1002/j.2637-496X.2018.tb01085.x
[4] Virey EH, Baron N. 45-1: status and prospects of microLED displays. SID Symp Dig Tech Papers. 2018;49(1):593. doi: 10.1002/sdtp.12415
[5] Chen F, Bian J, Hu J, et al. Mass transfer techniques for large-scale and high-density microLED arrays. Int J Extrem Manuf. 2022;4(4):042005. doi: 10.1088/2631-7990/ac92ee
[6] Beck VD, Piggin BP. Multiple-beam cathode ray tube design overview. IEEE Trans Electron Devices. 1986;33(8):1107. doi: 10.1109/t-ed.1986.22626
[7] Iniaghe PO, Adie GU. Management practices for end-of-life cathode ray tube glass: review of advances in recycling and best available technologies. Waste Manag Res. 2015;33(11):947. doi: 10.1177/0734242X15604212
[8] Heilmeier GH, Zanoni LA, Barton LA. Dynamic scattering: a new electrooptic effect in certain classes of nematic liquid crystals. Proc IEEE. 1968;56(7):1162. doi: 10.1109/proc.1968.6513
[9] Heilmeier GH, Zanoni LA, Barton LA. Dynamic scattering in nematic liquid crystals. Appl Phys Lett. 1968;13(1):46. doi: 10.1063/1.1652453

[10] Heilmeier GH, Zanoni LA, Barton LA. Further studies of the dynamic scattering mode in nematic liquid crystals. IEEE Trans Electron Devices. 1970;17(1):22. doi: 10.1109/t-ed.1970.16918
[11] Tang CW, VanSlyke SA. Organic electroluminescent diodes. Appl Phys Lett. 1987;51(12):913. doi: 10.1063/1.98799
[12] Yamazaki A, Wu CL, Cheng WC, et al. 33.2: spatial resolution characteristics of organic Light-emitting diode displays: a comparative analysis of MTF for handheld and workstation formats. SID Symp Dig Tech Papers. 2013;44(1):419. doi: 10.1002/j.2168-0159.2013.tb06236.x
[13] Lee J-H, Chen C-H, Lee P-H, et al. Blue organic light-emitting diodes: current status, challenges, and future outlook. J Mater Chem C. 2019;7(20):5874. doi: 10.1039/c9tc00204a
[14] Salehi A, Fu X, Shin DH, et al. Recent advances in OLED optical design. Adv Funct Mater. 2019;29(15). doi: 10.1002/adfm.201808803
[15] Chen HW, Lee JH, Lin BY, et al. Liquid crystal display and organic light-emitting diode display: present status and future perspectives. Light Sci Appl. 2018;7(3):17168. doi: 10.1038/lsa.2017.168
[16] Chen F, Qiu C, Liu Z. Investigation of autostereoscopic displays based on various display technologies. Nanomaterials (Basel). 2022;12(3):429. doi: 10.3390/nano12030429
[17] Chen D, Chen YC, Zeng G, et al. Integration technology of micro-LED for next-generation display. Research. 2023;6:0047. doi: 10.34133/research.0047
[18] Jin SX, Li J, Li JZ, et al. GaN microdisk light emitting diodes. Appl Phys Lett. 2000;76(5):631. doi: 10.1063/1.125841
[19] Jiang HX, Jin SX, Li J, et al. III-nitride blue microdisplays. Appl Phys Lett. 2001;78(9):1303. doi: 10.1063/1.1351521
[20] Ozden I, Diagne M, Nurmikko AV, et al. A matrix addressable 1024 element blue light emitting InGaN QW diode array. Physica Status Solidi (A). 2001;188(1):139. doi: 10.1002/1521-396x(200111)188:1<139:Aid-pssa139>3.0.Co;2-h
[21] Choi HW, Jeon CW, Dawson MD. High-resolution 128$times$96 nitride microdisplay. IEEE Electron Device Lett. 2004;25(5):277. doi: 10.1109/led.2004.826541
[22] Kim T-H, Cho K-S, Lee EK, et al. Full-colour quantum dot displays fabricated by transfer printing. Nat Photonics. 2011;5(3):176. doi: 10.1038/nphoton.2011.12
[23] Kim RH, Kim S, Song YM, et al. Flexible vertical light emitting diodes. Small. 2012;8(20):3123. doi: 10.1002/smll.201201195
[24] Bower CA, Meitl MA, Raymond B, et al. Emissive displays with transfer-printed assemblies of 8 μm × 15 μm inorganic light-emitting diodes. Photon Res. 2017;5(2):A23. doi: 10.1364/prj.5.000a23
[25] Henley FJ. 9.1: invited paper: materials, process and production equipment considerations to achieve High-Yield MicroLED Mass-production. SID Symp Dig Tech Papers. 2018;49(S1):86. doi: 10.1002/sdtp.12647
[26] Anderson R, Cohen D, Mehari S, et al. Electrical injection of a 440nm InGaN laser with lateral confinement by nanoporous-GaN. Opt Express. 2019;27(16):22764. doi: 10.1364/OE.27.022764
[27] Carreira JFC, Griffiths AD, Xie E, et al. Direct integration of micro-LEDs and a SPAD detector on a silicon CMOS chip for data communications and time-of-flight ranging. Opt Express. 2020;28(5):6909. doi: 10.1364/OE.384746
[28] Lin JY, Jiang HX. Development of microLED. Appl Phys Lett. 2020;116(10). doi: 10.1063/1.5145201
[29] Sheen M, Ko Y, Kim DU, et al. Highly efficient blue InGaN nanoscale light-emitting diodes. Nature. 2022;608(7921):56. doi: 10.1038/s41586-022-04933-5
[30] Lee JH, Ahn Y, Lee HE, et al. Wearable surface-lighting micro-light-emitting diode patch for melanogenesis inhibition. Adv Healthcare Materrials. 2023;12(1):e2201796. doi: 10.1002/adhm.202201796
[31] Lang T, Lin X, Huang X, et al. Thin-Film assisted laser transfer and bonding (TFA-LTAB) for the fabrication of Micro-LED displays. Adv Elect Mater. 2024;11(3). doi: 10.1002/aelm.202400380
[32] Bian J, Zhou L, Wan X, et al. Laser transfer, printing, and assembly techniques for flexible electronics. Adv Electron Mater. 2019;5(7). doi: 10.1002/aelm.201800900

[33] Huang Y, Tan G, Gou F, et al. Prospects and challenges of mini- LED and micro- LED displays. J Soc Info Disp. 2019;27(7):387. doi: 10.1002/jsid.760
[34] Kum H, Lee D, Kong W, et al. Epitaxial growth and layer-transfer techniques for heterogeneous integration of materials for electronic and photonic devices. Nat Electron. 2019;2 (10):439. doi: 10.1038/s41928-019-0314-2
[35] Zhou X, Tian P, Sher C-W, et al. Growth, transfer printing and colour conversion techniques towards full-colour micro-LED display. Prog Quantum Electron. 2020;71:100263. doi: 10.1016/j.pquantelec.2020.100263
[36] Hsiang EL, Yang Z, Yang Q, et al. Prospects and challenges of mini-LED, OLED, and micro-LED displays. J Soc Inf Disp. 2021;29(6):446. doi: 10.1002/jsid.1058
[37] Gong Y, Gong Z. Laser-Based Micro/Nano-processing techniques for microscale LEDs and Full-Color displays. Adv Mater Technol. 2022;8(5). doi: 10.1002/admt.202200949
[38] Zhu G, Liu Y, Ming R, et al. Mass transfer, detection and repair technologies in micro-LED displays. Sci China Mater. 2022;65(8):2128. doi: 10.1007/s40843-022-2110-2
[39] Ryu JE, Park S, Park Y, et al. Technological breakthroughs in chip fabrication, transfer, and color conversion for high-performance micro-LED displays. Adv Mater. 2023;35(43):e2204947. doi: 10.1002/adma.202204947
[40] Yu B, Li Y, Li J, et al. Challenges of high-yield manufacture in micro-light-emitting diodes displays: chip fabrication, mass transfer, and detection. J Phys D: Appl Phys. 2024;57 (46):463001. doi: 10.1088/1361-6463/ad6ce3
[41] Wu Y, Ma J, Su P, et al. Full-color realization of micro-LED displays. Nanomaterials (Basel). 2020;10(12):2482. doi: 10.3390/nano10122482
[42] Chen Z, Yan S, Danesh C. MicroLED technologies and applications: characteristics, fabrication, progress, and challenges. J Phys D: Appl Phys. 2021;54(12):123001. doi: 10.1088/1361-6463/abcfe4
[43] Li L, Tang G, Shi Z, et al. Transfer-printed, tandem microscale light-emitting diodes for full-color displays. Proc Natl Acad Sci U S A. 2021;118(18). doi: 10.1073/pnas.2023436118
[44] Carlson A, Bowen AM, Huang Y, et al. Transfer printing techniques for materials assembly and micro/nanodevice fabrication. Adv Mater. 2012;24(39):5284. doi: 10.1002/adma.201201386
[45] Yoon J, Lee SM, Kang D, et al. Heterogeneously integrated optoelectronic devices enabled by Micro-Transfer printing. Adv Optical Mater. 2015;3(10):1313. doi: 10.1002/adom.201500365
[46] Meitl MA, Radauscher E, Rotzoll R, et al. 19–4: invited paper: emissive displays with transfer-printed microscale inorganic LEDs. Symp Dig Tech Papers. 2017;48(1):257. doi: 10.1002/sdtp.11682
[47] Linghu C, Zhang S, Wang C, et al. Transfer printing techniques for flexible and stretchable inorganic electronics. Npj Flexible Electron. 2018;2(1). doi: 10.1038/s41528-018-0037-x
[48] Ding K, Avrutin V, Izyumskaya N, et al. Micro-LEDs, a manufacturability perspective. Appl Sci. 2019;9(6):1206. doi: 10.3390/app9061206
[49] Ezhilarasu G, Hanna A, Paranjpe A, et al. High yield precision transfer and assembly of GaN μLEDs using laser assisted micro transfer printing. In: IEEE 69th electronic components and technology conference. New York City (USA): IEEE; 2019. p. 1470–1477.
[50] Bower CA, Bonafede S, Radauscher E, et al. Emissive displays with transfer-printed microscale LEDs and ICs. Light-Emitting Devices, Mater, Appl XXIV, Vol. 11302. 2020. p. 1130202.
[51] Chen Z, Zhang C, Zheng Z. Advancements in transfer printing techniques for flexible electronics: adjusting interfaces and promoting versatility. Int J Extrem Manuf. 2024;6(5):052005. doi: 10.1088/2631-7990/ad5391
[52] Zhao J, Xia N, Zhang L. A review of bioinspired dry adhesives: from achieving strong adhesion to realizing switchable adhesion. Bioinspir Biomim. 2024;19(5):051003. doi: 10.1088/1748-3190/ad62cf
[53] Linghu C, Mu T, Zhao W, et al. Advancing smart dry adhesives with shape memory polymers. Int J Smart Nano Mater. 2024;16(1):103–143. doi: 10.1080/19475411.2024.2439954
[54] Park T, Kim JS, Ko D, et al. Advances in flexible, foldable, and stretchable quantum dot light-emitting diodes: materials and fabrication strategies. Korean J Chem Eng. 2024;41 (13):3517. doi: 10.1007/s11814-024-00236-9

[55] Park SY, Lee S, Yang J, et al. Patterning quantum dots via photolithography: a review. Adv Mater. 2023;35(41):e2300546. doi: 10.1002/adma.202300546
[56] Pan Z-J, Chen Z-Z, Jiao F, et al. A review of key technologies for epitaxy and chip process of micro light-emitting diodes in display application. Acta Phys Sin. 2020;69(19):198501. doi: 10.7498/aps.69.20200742
[57] Li ZT, Li JX, Zheng JL, et al. Review of quantum dot-based LED display: materials, encapsulation coatings, patterned display applications. Chin J Liquid Cryst Disp. 2023;38(3):319. doi: 10.37188/cjlcd.2022-0361
[58] Li KH, Fu WY, Choi HW. Chip-scale GaN integration. Prog Quantum Electron. 2020;70:100247. doi: 10.1016/j.pquantelec.2020.100247
[59] Lee GH, Kim K, Kim Y, et al. Recent advances in patterning strategies for full-color perovskite light-emitting diodes. Nano-Micro Lett. 2023;16(1):45. doi: 10.1007/s40820-023-01254-8
[60] Shet S, Revero RD, Booty MR, et al. Microassembly techniques: a review. Mater Sci Technol 2006 Proc. 2006;1:451.
[61] Wong WS, Sands T, Cheung NW. Damage-free separation of GaN thin films from sapphire substrates. Appl Phys Lett. 1998;72(5):599. doi: 10.1063/1.120816
[62] Hyun Kyong C, Sun-Kyung K, Duk Kyu B, et al. Laser liftoff GaN thin-film photonic crystal GaN-based light-emitting diodes. IEEE Photon Technol Lett. 2008;20(24):2096. doi: 10.1109/lpt.2008.2006506
[63] Chen LC, Wang CK, Huang JB, et al. A nanoporous AlN layer patterned by anodic aluminum oxide and its application as a buffer layer in a GaN-based light-emitting diode. Nanotechnology. 2009;20(8):085303. doi: 10.1088/0957-4484/20/8/085303
[64] Lin C-F, Dai J-J, Lin M-S, et al. An AlN sacrificial Buffer Layer inserted into the GaN/Patterned sapphire substrate for a chemical lift-off process. Appl Phys Express. 2010;3(3):031001. doi: 10.1143/apex.3.031001
[65] Ueda T, Ishida M, Yuri M. Separation of thin GaN from sapphire by laser lift-off technique. Jpn J Appl Phys. 2011;50(4R):041001. doi: 10.1143/jjap.50.041001
[66] Wang MQ, Wang Y, Sun YJ, et al. Thermo-mechanical solution of film/substrate systems under local thermal load and application to laser lift-off of GaN/sapphire structures. Int J Solids Struct. 2012;49(13):1701. doi: 10.1016/j.ijsolstr.2012.03.011
[67] Chuang S-H, Pan C-T, Shen K-C, et al. Thin film GaN LEDs using a patterned oxide sacrificial Layer by chemical lift-off process. IEEE Photonic Tech L. 2013;25(24):2435. doi: 10.1109/lpt.2013.2287892
[68] Park J, Sin Y-G, Kim J-H, et al. Dependence of adhesion strength between GaN LEDs and sapphire substrate on power density of UV laser irradiation. Appl Surf Sci. 2016;384:353. doi: 10.1016/j.apsusc.2016.05.078
[69] Bornemann S, Yulianto N, Meyer T, et al. Structural modifications in free-standing InGaN/GaN LEDs after femtosecond laser lift-off. Proceedings. 2018;2(13):897. doi: 10.3390/proceedings2130897
[70] Singh AK, Ahn K, Yoo D, et al. van der Waals integration of GaN light-emitting diode arrays on foreign graphene films using semiconductor/graphene heterostructures. NPG Asia Mater. 2022;14(1). doi: 10.1038/s41427-022-00403-6
[71] Linghu C, Zhang S, Wang C, et al. Mass transfer for micro-LED display: transfer printing techniques. In: Jiang H, Lin J, editors. Semiconductors and Semimetals. Vol. 106. Netherlands: Elsevier; 2021. p. 253–280.
[72] Carlson A, Wang S, Elvikis P, et al. Active, programmable elastomeric surfaces with tunable adhesion for deterministic assembly by transfer printing. Adv Funct Mater. 2012;22(21):4476. doi: 10.1002/adfm.201201023
[73] Ahmed N, Dagdeviren C, Rogers JA, et al. Active polymeric composite membranes for localized actuation and sensing in microtransfer printing. J Microelectromech Syst. 2014;24(4):1016. doi: 10.1109/JMEMS.2014.2375811
[74] Bower CA, Meitl MA, Bonafede S, et al. Heterogeneous integration of microscale compound semiconductor devices by micro-transfer-printing. In: 2015 IEEE 65th electronic components and technology conference. New York City (USA): IEEE. 2015. p. 963–967.

[75] Trindade AJ, Guilhabert B, Xie EY, et al. Heterogeneous integration of gallium nitride light-emitting diodes on diamond and silica by transfer printing. Opt Express. 2015;23 (7):9329. doi: 10.1364/OE.23.009329
[76] Cho S, Kim N, Song K, et al. Adhesiveless transfer printing of ultrathin microscale semiconductor materials by controlling the bending radius of an elastomeric stamp. Langmuir. 2016;32(31):7951. doi: 10.1021/acs.langmuir.6b01880
[77] Linghu C, Wang C, Cen N, et al. Rapidly tunable and highly reversible bio-inspired dry adhesion for transfer printing in air and a vacuum. Soft Matter. 2018;15(1):30. doi: 10.1039/c8sm01996g
[78] Pan Z, Guo C, Wang X, et al. Wafer-Scale Micro-LEDs transferred onto an adhesive film for planar and flexible displays. Adv Mater Technol. 2020;5(12). doi: 10.1002/admt.202000549
[79] Lu X, Zhu S, Lin R, et al. Performance improvement of red InGaN micro-LEDs by transfer printing from Si substrate onto glass substrate. IEEE Electron Device Lett. 2022;43(9):1491. doi: 10.1109/led.2022.3189443
[80] Sun W, Ji L, Lin Z, et al. 20 microm micro-LEDs Mass transfer via laser-induced in situ nanoparticles resonance enhancement. Small. 2024;20(27):e2309877. doi: 10.1002/smll.202309877
[81] Yoo J, Lee K, Yang UJ, et al. Highly efficient printed quantum dot light-emitting diodes through ultrahigh-definition double-layer transfer printing. Nat Photon. 2024;18 (10):1105–1112. doi: 10.1038/s41566-024-01496-x
[82] Zhai P, Xie B, Xu Z, et al. Simulation and experimental analysis of contactless chip pickup process based on a vortex flow gripper. IEEE Transactions on Semiconductor Manufacturing. 2024;38(2):324–331. doi: 10.1109/TSM.2025.3553559
[83] Hwang K, Hwang J, Kim Y, et al. 1.6-inch transparent micro-display with pixel circuit integrated microLED chip array by Misalignment-Free Transfer. Adv Mater. 2025;37(9):e2416015. doi: 10.1002/adma.202416015
[84] Zhao J, Lu T, Pan T, et al. Mushroom-shaped micropillar with a maximum pull-off force. J Appl Mech. 2022;89(7). doi: 10.1115/1.4054628
[85] Zhang Y, Lu T, Zhao J, et al. Mechanics of transfer printing for elastomeric stamps with collapse cavities. Extrem Mech Lett. 2023;60:60. doi: 10.1016/j.eml.2023.101956
[86] Wang Y, Zhao J, He Y, et al. Contact stiffness of the multi-indenter contact interface. J Mech Phys Solids. 2024;188:105659. doi: 10.1016/j.jmps.2024.105659
[87] Linghu C, Zhu H, Zhu J, et al. Mechanics of magnet-controlled transfer printing. Extrem Mech Lett. 2019;27:76. doi: 10.1016/j.eml.2019.01.006
[88] Meitl MA, Zhu Z-T, Kumar V, et al. Transfer printing by kinetic control of adhesion to an elastomeric stamp. Nat Mater. 2006;5(1):33. doi: 10.1038/nmat1532
[89] Feng X, Meitl MA, Bowen AM, et al. Competing fracture in kinetically controlled transfer printing. Langmuir. 2007;23(25):12555. doi: 10.1021/la701555n
[90] Park SI, Xiong Y, Kim RH, et al. Printed assemblies of inorganic light-emitting diodes for deformable and semitransparent displays. Science. 2009;325(5943):977. doi: 10.1126/science.1175690
[91] Kim-Lee HJ, Carlson A, Grierson DS, et al. Interface mechanics of adhesiveless microtransfer printing processes. J Appl Phys. 2014;115(14). doi: 10.1063/1.4870873
[92] Kim S, Wu J, Carlson A, et al. Microstructured elastomeric surfaces with reversible adhesion and examples of their use in deterministic assembly by transfer printing. Proc Natl Acad Sci U S A. 2010;107(40):17095. doi: 10.1073/pnas.1005828107
[93] Yang SY, Carlson A, Cheng H, et al. Elastomer surfaces with directionally dependent adhesion strength and their use in transfer printing with continuous roll-to-roll applications. Adv Mater. 2012;24(16):2117. doi: 10.1002/adma.201104975
[94] Yang Y, Hwang Y, Cho HA, et al. Arrays of silicon micro/nanostructures formed in suspended configurations for deterministic assembly using flat and roller-type stamps. Small. 2011;7 (4):484. doi: 10.1002/smll.201001633

[95] Ahn SH, Guo LJ. Large-area roll-to-roll and roll-to-plate nanoimprint lithography: a step toward high-throughput application of continuous nanoimprinting. ACS Nano. 2009;3 (8):2304. doi: 10.1021/nn9003633
[96] Bae S, Kim H, Lee Y, et al. Roll-to-roll production of 30-inch graphene films for transparent electrodes. Nat Nanotechnol. 2010;5(8):574. doi: 10.1038/nnano.2010.132
[97] Tavares L, Kjelstrup-Hansen J, Rubahn HG. Efficient roll-on transfer technique for well-aligned organic nanofibers. Small. 2011;7(17):2460. doi: 10.1002/smll.201100660
[98] Sharma BK, Jang B, Lee JE, et al. Load-Controlled roll transfer of oxide transistors for stretchable electronics. Adv Funct Mater. 2012;23(16):2024. doi: 10.1002/adfm.201202519
[99] Park SC, Biswas S, Fang J, et al. Millimeter thin and rubber-like solid-state lighting modules fabricated using roll-to-roll fluidic self-assembly and lamination. Adv Mater. 2015;27(24):3661. doi: 10.1002/adma.201500839
[100] Plochowietz A, Wang YD, Shreve M, et al. Programmable micro-object assembly with transfer. In: 20th international conference on solid-state sensors, actuators and microsystems & eurosensors xxxiii. New York City (USA): IEEE. 2019. p. 390–393.
[101] Rupp BB, Plochowietz A, Crawford LS, et al. Chiplet Micro-Assembly Printer. In: IEEE 69th electronic components and technology conference. New York City (USA): IEEE. 2019. p. 1312–1315.
[102] Lee SH, Lee S. Fabrication of comb-structured acceleration sensors by roll-to-roll gravure printing. Int J Precis Eng Manuf Green Tech. 2021;9(2):409. doi: 10.1007/s40684-021-00342-7
[103] Margariti E, Quinn G, Jevtics D, et al. Continuous roller transfer-printing and automated metrology of >75,000 micro-LED pixels in a single shot. Opt Mater Express. 2023;13(8):2236. doi: 10.1364/ome.483657
[104] Yoon SU, Hwangbo Y, Jang B, et al. Transfer of Micro-LEDs with Roll-Based direct overlay alignment for manufacturing transparent displays. Adv Elect Mater. 2024;10(11). doi: 10.1002/aelm.202400236
[105] Choi M, Jang B, Lee W, et al. Stretchable active matrix inorganic Light-Emitting diode display enabled by Overlay-Aligned Roll-Transfer printing. Adv Funct Mater. 2017;27(11). doi: 10.1002/adfm.201606005
[106] Nam TW, Kim M, Wang Y, et al. Thermodynamic-driven polychromatic quantum dot patterning for light-emitting diodes beyond eye-limiting resolution. Nat Commun. 2020;11(1):3040. doi: 10.1038/s41467-020-16865-7
[107] Bail R, Ma SY, Lee DH. Additive manufacturing of a micropatterned stamp for transfer printing of quantum dots. J Photopolym Sci Tec. 2021;34(6):651. doi: 10.2494/photopolymer.34.651
[108] Xiao Z, Zhang M, Ding Y, et al. Solution-processed quantum dot micropatterns: from liquid manipulation to high-performance quantum dot light-emitting diode devices. ACS Nano. 2025;19(11):10609. doi: 10.1021/acsnano.5c01172
[109] Chen Z, Li H, Yuan C, et al. Color revolution: prospects and challenges of quantum-dot light-emitting diode display technologies. Small Methods. 2024;8(2):e2300359. doi: 10.1002/smtd.202300359
[110] Yang K, Zheng H, Zhong C, et al. High-resolution and high-performance full-color electroluminescent quantum dot light-emitting diodes. Nano Energy. 2025;138:110817. doi: 10.1016/j.nanoen.2025.110817
[111] Kwon JI, Park G, Lee GH, et al. Ultrahigh-resolution full-color perovskite nanocrystal patterning for ultrathin skin-attachable displays. Sci Adv. 2022;8(43):eadd0697. doi: 10.1126/sciadv.add0697
[112] Lee J, Kim Y, Lee K, et al. Transfer-printed multi-stacked quantum dot color conversion layers for white light-emitting diodes. Appl Surf Sci. 2025;687:687. doi: 10.1016/j.apsusc.2024.162196
[113] Choi MK, Yang J, Kang K, et al. Wearable red–green–blue quantum dot light-emitting diode array using high-resolution intaglio transfer printing. Nat Commun. 2015;6(1):7149. doi: 10.1038/ncomms8149
[114] Kim BH, Nam S, Oh N, et al. Multilayer transfer printing for pixelated, multicolor quantum dot light-emitting diodes. ACS Nano. 2016;10(5):4920. doi: 10.1021/acsnano.5b06387
[115] Meng T, Zheng Y, Zhao D, et al. Ultrahigh-resolution quantum-dot light-emitting diodes. Nat Photonics. 2022;16(4):297. doi: 10.1038/s41566-022-00960-w

[116] Tavernier PR, Clarke DR. Mechanics of laser-assisted debonding of films. J Appl Phys. 2001;89 (3):1527. doi: 10.1063/1.1338519
[117] Marinov VR, Swenson O, Atanasov Y, et al. Laser-assisted ultrathin die packaging: insights from a process study. Microelectronic Eng. 2013;101:23. doi: 10.1016/j.mee.2012.08.016
[118] Li J, Liu Z. P-10.1: transfer process of micro-LED using laser. Symp Dig Tech Papers. 2023;54 (S1):787. doi: 10.1002/sdtp.16412
[119] Saeidpourazar R, Li R, Li Y, et al. Laser-driven micro transfer placement of prefabricated microstructures. J Microelectromech Syst. 2012;21(5):1049. doi: 10.1109/jmems.2012.2203097
[120] Saeidpourazar R, Sangid MD, Rogers JA, et al. A prototype printer for laser driven micro-transfer printing. J Manuf Processes. 2012;14(4):416. doi: 10.1016/j.jmapro.2012.09.014
[121] Li R, Li Y, Lü C, et al. Thermo-mechanical modeling of laser-driven non-contact transfer printing: two-dimensional analysis. Soft Matter. 2012;8(27):7122. doi: 10.1039/c2sm25339a
[122] Li R, Li Y, Lü C, et al. Axisymmetric thermo-mechanical analysis of laser-driven non-contact transfer printing. Int J Fract. 2012;176(2):189. doi: 10.1007/s10704-012-9744-9
[123] AaM A-O, Rogers JA, Ferreira PM. Characterization of delamination in laser microtransfer printing. J Micro Nano-Manuf. 2014;2(1). doi: 10.1115/1.4026238
[124] Gao Y, Li Y, Li R, et al. An accurate thermomechanical Model for laser-driven microtransfer printing. J Appl Mech. 2017;84(6). doi: 10.1115/1.4036257
[125] Li Z, Li Z, Li J, et al. Manufacturing carbon-doped stamp with surface microstructures for rapid and reliable micro-LED transfer process. IEEE Trans Electron Devices. 2025;72(2):749. doi: 10.1109/ted.2024.3519493
[126] Bohandy J, Kim BF, Adrian FJ. Metal deposition from a supported metal film using an excimer laser. J Appl Phys. 1986;60(4):1538. doi: 10.1063/1.337287
[127] Delaporte P, Alloncle A-P. [INVITED] laser-induced forward transfer: a high resolution additive manufacturing technology. Optics Laser Technol. 2016;78:33. doi: 10.1016/j.optlastec.2015.09.022
[128] Um JG, Jeong DY, Jung Y, et al. Active-Matrix GaN μ-LED display using oxide Thin-Film transistor backplane and flip chip LED bonding. Adv Elect Mater. 2018;5(3). doi: 10.1002/aelm.201800617
[129] Lee D, Cherekdjian S, Kang S, et al. 18-2: Ultra-Fine high efficiency MicroLEDs with testability and transferability using Layer-Transfer technology. SID Symp Dig Tech Papers. 2019;50 (1):236. doi: 10.1002/sdtp.12899
[130] Holmes AS, Saidam SM. Sacrificial layer process with laser-driven release for batch assembly operations. J Microelectromech Syst. 1998;7(4):416. doi: 10.1109/84.735350
[131] Karnakis DM, Lippert T, Ichinose N, et al. Laser induced molecular transfer using ablation of a triazeno-polymer. Appl Surf Sci. 1998;127:781. doi: 10.1016/S0169-4332(97)00742-3
[132] Voronenkov V, Bochkareva N, Gorbunov R, et al. Laser slicing: a thin film lift-off method for GaN-on-GaN technology. Results Phys. 2019;13:102233. doi: 10.1016/j.rinp.2019.102233
[133] Marinov V, Swenson O, Miller R, et al. Laser-enabled advanced packaging of ultrathin bare dice in flexible substrates. IEEE Trans Comp Packag Manuf Technol. 2012;2(4):569. doi: 10.1109/tcpmt.2011.2176941
[134] Miller R, Marinov V, Swenson O, et al. Noncontact selective laser-assisted placement of thinned semiconductor dice. IEEE Trans Comp Packag Manuf Technol. 2012;2(6):971. doi: 10.1109/tcpmt.2012.2183594
[135] Marinov VR. 52-4: Laser-Enabled Extremely-High rate technology for μLED assembly. SID Symp Dig Tech Papers. 2018;49(1):692. doi: 10.1002/sdtp.12352
[136] Luo H, Wang C, Linghu C, et al. Laser-driven programmable non-contact transfer printing of objects onto arbitrary receivers via an active elastomeric microstructured stamp. Natl Sci Rev. 2020;7(2):296. doi: 10.1093/nsr/nwz109
[137] Wang C, Linghu C, Nie S, et al. Programmable and scalable transfer printing with high reliability and efficiency for flexible inorganic electronics. Sci Adv. 2020;6(25):eabb2393. doi: 10.1126/sciadv.abb2393
[138] Chen F, Gai M, Sun N, et al. Laser-driven hierarchical “gas-needles” for programmable and high-precision proximity transfer printing of microchips. Sci Adv. 2023;9(43):eadk0244. doi: 10.1126/sciadv.adk0244

[139] Zheng N, Fang G, Cao Z, et al. High strain epoxy shape memory polymer. Polym Chem. 2015;6(16):3046. doi: 10.1039/c5py00172b
[140] Zhang S, Wang C, Nie S, et al. Wrinkling of silicon nanoribbons on shape memory polymers. J Phys D: Appl Phys. 2019;52(26):265101. doi: 10.1088/1361-6463/ab188a
[141] Eisenhaure J, Kim S. Laser-Driven shape memory effect for transfer printing combining parallelism with individual object control. Adv Mater Technol. 2016;1(7). doi: 10.1002/admt.201600098
[142] Eisenhaure JD, Rhee SI, AaM A-O, et al. The use of shape memory polymers for MEMS assembly. J Microelectromech Syst. 2016;25(1):69. doi: 10.1109/jmems.2015.2482361
[143] Linghu C, Zhang S, Wang C, et al. Universal SMP gripper with massive and selective capabilities for multiscaled, arbitrarily shaped objects. Sci Adv. 2020;6(7):eaay5120. doi: 10.1126/sciadv.aay5120
[144] Linghu C, Liu Y, Tan YY, et al. Overcoming the adhesion paradox and switchability conflict on rough surfaces with shape-memory polymers. Proc Natl Acad Sci U S A. 2023;120(13):e2221049120. doi: 10.1073/pnas.2221049120
[145] Li C, Zhang S, Jiang J, et al. Laser-induced adhesives with excellent adhesion enhancement and reduction capabilities for transfer printing of microchips. Sci Adv. 2024;10(49):eads9226. doi: 10.1126/sciadv.ads9226
[146] Ashdown I, Speier I, Sheen CW, et al. Method and magnetic transfer stamp for transferring semiconductor dice using magnetic transfer printing techniques. United States Patent. 2011.
[147] Ashdown I, Speier I. Method and eletrostatic transfer stamp for transferring semiconductor dice using electrostatic transfer printing techniques. United States Patent. 2015.
[148] Wu M-H, Fang Y-H, Chao C-H. Magnetic transfer module and method for transferring electronic element. United States Patent. 2020.
[149] Zhao J, Li X, Tan Y, et al. Smart adhesives via magnetic actuation. Adv Mater. 2022;34(8):e2107748. doi: 10.1002/adma.202107748
[150] Zhao J, Lu T, Zhang Y, et al. Magnetically actuated adhesives with switchable adhesion. Adv Funct Mater. 2023;33(52):2305484. doi: 10.1002/adfm.202305484
[151] Bibl A, Higginson JA, Law H-F, et al. Method of transferring a micro device. United States Patent. 2012.
[152] Bibl A, Higginson JA, Law H-F, et al. Micro device transfer head heater assembly and method of transferring a micro device. United States Patent. 2013.
[153] Hu H-H, Bibl A, Higginson JA, et al. Method of fabricating and transferring a micro device and an array of micro devices utilizing an intermediate electrically conductive bonding layer. United States Patent. 2013.
[154] Bibl A, Higginson JA, Law H-F, et al. Micro device transfer head heater assembly and method of transferring a micro device. United States Patent. 2014.
[155] Bibl A, Golda D. Micro pick up array with compliant contact. United States Patent. 2015.
[156] Bibl A, Higginson JA, Hu H-H, et al. Method of transferring and bonding an array of micro devices. United States patent. 2017.
[157] Kim S, Jiang Y, Thompson Towell KL, et al. Soft nanocomposite electroadhesives for digital micro- and nanotransfer printing. Sci Adv. 2019;5(10):eaax4790. doi: 10.1126/sciadv.aax4790
[158] Ming-Hsien W, Yen-Hsiang F, Chia-Hsin C. Electric-programmable magnetic module and picking-up and placement process for electronic devices. United States patent. 2017.
[159] Valentine AD, Busbee TA, Boley JW, et al. Hybrid 3D printing of soft electronics. Adv Mater. 2017;29(40). doi: 10.1002/adma.201703817
[160] Yamashita T, Takamatsu S, Okada H, et al. Development of flexible piezoelectric strain sensor array. Electr Eng Jpn. 2018;204(1):52. doi: 10.1002/eej.23084
[161] Yeong-Jyh L, Sheng-Jye H. Static analysis of the die picking process. IEEE Trans Electron Packag Manufact. 2005;28(2):142. doi: 10.1109/tepm.2005.847396
[162] Peng B, Huang Y, Yin Z, et al. Competing fracture modeling of thin chip pick-up process. IEEE Trans Comp Packag Manuf Technol. 2012;2(7):1217. doi: 10.1109/tcpmt.2012.2197859
[163] Cheng T-H, Du C-C, Tseng C-H. Study in IC chip failure during pick-up process by using experimental and finite element methods. J Mater Process Technol. 2006;172(3):407. doi: 10.1016/j.jmatprotec.2005.11.002

[164] Liu H, Liu Z, Xu Z, et al. Competing fracture of thin-chip transferring From/Onto prestrained compliant substrate. J Appl Mech. 2015;82(10). doi: 10.1115/1.4031047
[165] Park SH, Kim TJ, Lee HE, et al. Universal selective transfer printing via micro-vacuum force. Nat Commun. 2023;14(1):7744. doi: 10.1038/s41467-023-43342-8
[166] Ji L, Zhang G, Zhang J, et al. An alternative micro LED Mass transfer technology: self-assembly. In: 23rd International conference on electronic packaging technology. New York City (USA): IEEE. 2022. p. 1–5.
[167] Eo YJ, Yoo GY, Kang H, et al. Enhanced DC-Operated electroluminescence of forwardly aligned p/MQW/n InGaN nanorod LEDs via DC offset-AC dielectrophoresis. ACS Appl Mater Interfaces. 2017;9(43):37912. doi: 10.1021/acsami.7b09794
[168] Shetye SB, Eskinazi I, Arnold DP. Self-assembly of millimeter-scale components using integrated micromagnets. IEEE Trans Magn. 2008;44(11):4293. doi: 10.1109/tmag.2008.2001344
[169] Yeh HJJ, Smith JS. Fluidic self-assembly for the integration of gaas light-emitting-diodes on Si substrates. IEEE Photonic Tech L. 1994;6(6):706. doi: 10.1109/68.300169
[170] Talghader JJ, Tu JK, Smith JS. Integration of fluidically self-assembled optoelectronic devices using a silicon-based process. IEEE Photonic Tech L. 1995;7(11):1321. doi: 10.1109/68.473485
[171] Schuele PJ, Sasaki K, Ulmer K, et al. Display with surface mount emissive elements. United States patent. 2017.
[172] Sasaki K, Schuele P, Ulmer K, et al. System and method for the fluidic assembly of emissive displays. United States Patent. 2019.
[173] Stauth SA, Parviz BA. Self-assembled single-crystal silicon circuits on plastic. Proc Natl Acad Sci U S A. 2006;103(38):13922. doi: 10.1073/pnas.0602893103
[174] Kaltwasser M, Schmidt U, Lösing L, et al. Fluidic self-assembly on electroplated multilayer solder bumps with tailored transformation imprinted melting points. Sci Rep. 2019;9(1). doi: 10.1038/s41598-019-47690-8
[175] Park M, Yoo B, Hong M, et al. Optimizing binding site spacing in fluidic self-assembly for enhanced microchip integration density. Micromachines (Basel). 2024;15(3):300. doi: 10.3390/mi15030300
[176] Böhringer KF, Srinivasan U, Howe RT. Modeling of capillary forces and binding sites for fluidic self-assembly. In: 14th IEEE international conference on micro electro mechanical systems. New York City (USA): IEEE. 2001. p. 369–374.
[177] Srinivasan U, Liepmann D, Howe RT. Microstructure to substrate self-assembly using capillary forces. J Microelectromech Syst. 2001;10(1):17. doi: 10.1109/84.911087
[178] Morris CJ, Parviz BA. Micro-scale system integration via molten-alloy driven self-assembly and scaling of metal interconnects. In: The 14th international conference on solid-state sensors, actuators and microsystems. New York City (USA): IEEE. 2007. p. 411–414.
[179] Morris CJ, Parviz BA. Micro-scale metal contacts for capillary force-driven self-assembly. J Micromech Microeng. 2008;18(1):015022. doi: 10.1088/0960-1317/18/1/015022
[180] Lee D, Cho S, Park C, et al. Fluidic self-assembly for MicroLED displays by controlled viscosity. Nature. 2023;619(7971):755. doi: 10.1038/s41586-023-06167-5
[181] O'Riordan A, Delaney P, Redmond G. Field configured assembly: programmed manipulation and self-assembly at the mesoscale. Nano Lett. 2004;4(5):761. doi: 10.1021/nl034145q
[182] Lee SW, Bashir R. Dielectrophoresis and chemically mediated directed Self-Assembly of Micrometer-Scale Three-Terminal metal oxide semiconductor Field-Effect transistors. Adv Mater. 2005;17(22):2671. doi: 10.1002/adma.200501048
[183] Park HK, Yoon SW, Eo YJ, et al. Horizontally assembled green InGaN nanorod LEDs: scalable polarized surface emitting LEDs using electric-field assisted assembly. Sci Rep. 2016;6(1):28312. doi: 10.1038/srep28312
[184] Chang W, Kim J, Kim M, et al. Concurrent self-assembly of RGB microLEDs for next-generation displays. Nature. 2023;617(7960):287. doi: 10.1038/s41586-023-05889-w